Towards a high quality in-situ observation network for oxygenated volatile organic compounds (OVOCs) in Europe: transferring traceability to the International System of Units (SI) to the field

Maitane Iturrate-Garcia[1], Thérèse Salameh[2], Paul Schlauri[3], Annarita Baldan[4], Martin K. Vollmer[3], Evdokia Stratigou[2], Sebastian Dusanter[2], Jianrong Li[4], Stefan Persijn[4], Anja Claude[5], Rupert Holzinger[6], Christophe Sutour[7], Tatiana Macé[7], Yasin Elshorbany[8], Andreas Ackermann[1], Céline Pascale[1], Stefan Reimann[3]

[1] Department of Chemical and Biological Metrology, Federal Institute of Metrology (METAS), Bern-Wabern, 3003, Switzerland
[2] IMT Nord Europe, Institute Mines-Télécom, Univ. Lille, Centre for Energy and Environment, F-59000 Lille, France
[3] Laboratory for Air Pollution and Environmental Technology, Empa, Swiss Federal Laboratories for Materials Science and Technology, Dübendorf, 8600, Switzerland
[4] VSL-National Metrology Institute, Delft, 2629 JA, the Netherlands
[5] Meteorologisches Observatorium Hohenpeissenberg, Deutscher Wetterdienst (DWD), 82383 Hohenpeissenberg, Germany
[6] Institute for Marine and Atmospheric Research, IMAU, Utrecht University, Utrecht, the Netherlands
[7] Department of Gas Metrology, Laboratoire National de Métrologie et d'Essais – LNE, Paris CEDEX 15, 75724, France
[8] School of Geosciences, College of Arts & Sciences, University of South Florida, Florida, USA

Correspondence to: Maitane Iturrate-Garcia (maitane.iturrate@metas.ch)

Abstract. Volatile organic compounds (VOCs) have a large impact on the oxidising capacity of the troposphere and are major precursors of tropospheric ozone and secondary atmospheric aerosols. Accurate measurements and data comparability of VOCs among monitoring networks are essential to assess the trends of these secondary air pollutants. Metrological traceability of the measurements to the international system of units (SI-traceability) contributes to both: measurement consistency and data comparability. Accurate, stable and SI-traceable reference gas mixtures (RGMs) and working standards are needed to achieve SI-traceability through an unbroken chain of calibrations of the analytical instruments used to monitor VOCs. However, for many oxygenated VOCs (OVOCs), such RGMs and working standards are not available at atmospheric amount of substance fraction levels (< 10 nmol mol^{-1}). Here, we present the protocols developed to transfer SI-traceability to the field by producing two types of SI-traceable working standards for selected OVOCs. These working standards, based on RGMs diluted dynamically with dry nitrogen and on certified spiked whole air samples, were then assessed using Thermal Desorption-Gas Chromatography-Flame Ionization Detector (TD-GC-FID) and Proton Transfer Reaction-Time of Flight-Mass Spectrometry (PTR-ToF-MS) as analytical methods. For that purpose, we calibrated five analytical instruments using in-house calibration standards and treated the new SI-traceable working standards as samples. Due to analytical limitations, the assessment was only possible for acetaldehyde, acetone, methanol and methyl ethyl ketone (MEK). Relative differences between assigned and measured values were used to assess the working standards based on dilution of RGMs. The relative differences were within the measurement uncertainty for acetone, MEK, methanol and acetaldehyde at amount of substance

35 fractions around 10 nmol mol^{-1}. For the working standards based on certified spiked whole air samples in pressurized cylinders, results showed a good agreement among the laboratories (i.e., differences within the measurement expanded uncertainties (U) ranging between 0.5 nmol mol^{-1} and 3.3 nmol mol^{-1}) and with the certified amount of substance fraction value for acetaldehyde (15.7 nmol mol^{-1} ± 3.6 (U) nmol mol^{-1}), acetone (17 nmol mol^{-1} ± 1.5 (U) nmol mol^{-1}) and MEK (12.3 nmol mol^{-1} ± 2.3 (U) nmol mol^{-1}). Despite the promising results for the working standards based on the dilution of RGMs and on certified spiked

40 whole air samples filled into pressurized cylinders, the assessment must be considered with care due to the large measurement uncertainty, particularly for methanol. Active collaboration among metrological, meteorological and atmospheric chemistry monitoring communities is needed to tackle the challenges of OVOC monitoring, such as the lack of stable and SI-traceable calibration standards (i.e., RGMs and working standards). Besides from this collaboration, other research applications, such as modelling and remote sensing, may benefit from the transfer of SI-traceability to monitoring stations.

Keywords

Calibration, metrological traceability, uncertainty, VOCs, tropospheric ozone, reference gas mixtures, GC-FID, PTR-MS

1 Introduction

Tropospheric ozone plays a key role in the oxidative capacity of the atmosphere (Monks et al., 2015; Schultz et al., 2015;

50 Iglesias-Suarez et al., 2018). Despite its relatively low atmospheric abundance and short lifetime (20–25 days or even lower) (Young et al., 2013), ozone photodissociation is the dominant source of hydroxyl radical (OH) in the troposphere (e.g., Lelieveld and Dentener, 2000; Zhang et al., 2014). Besides being a strong oxidant with direct impact on human respiratory health, vegetation growth and crop productivity (Van Dingenen et al., 2009; Schultz et al., 2017; Mills et al., 2018), tropospheric ozone is also a greenhouse gas and a secondary air pollutant. In the troposphere, ozone abundance depends on its

55 transport from the stratosphere, formation and destruction through photochemical reactions and dry deposition (Jacob, 2000; Stohl et al., 2003; Wild, 2007; Cooper et al., 2014). Volatile organic compounds (VOCs) – a group of chemical compounds with one or more atoms of carbon and a complex speciation that encompasses thousands of species (Goldstein and Galbally, 2007; Yang et al., 2016) – are one of the major tropospheric ozone precursors (Shao et al., 2009; Xue et al., 2014; Simon et al., 2015). VOC oxidation in the presence of significant amount of substance fractions of nitrogen oxides (NO$_x$) results in a

60 net production of ozone (Collins et al., 2002; Pugliese et al., 2014).

Oxygenated VOCs (OVOCs) are an important fraction of VOCs, which includes alcohols, carbonyls (aldehydes and ketones) and carboxylic acid (Legreid et al., 2007; Wu et al., 2020). OVOCs are precursors of tropospheric ozone and secondary organic aerosols and have, thus, an impact on air quality and climate (Boucher et al., 2013; Seinfeld et al., 2016; Shrivasta et al., 2017). OVOCs can be formed by atmospheric photooxidation of hydrocarbons (Atkinson, 2000) and can be emitted directly from

65 vegetation, biomass burning, vehicle exhaust and industrial processes (Placet, 2000; Legreid et al., 2007; Worton et al., 2022). OVOCs with low molecular weights (e.g., methanol, acetone, acetaldehyde, methyl ethyl ketone (MEK)) are found at relatively

high amount of substance fractions in the global atmosphere and play and important role in the tropospheric photochemistry. For these OVOCs, the main sinks are the oxidation with the OH radical and degradation initiated by photolysis leading to the formation of hydrogen oxide radicals (HO_x). For example, oxidation products of methanol are formaldehyde and CO (Hu et al., 2011; Bates et al., 2021), which also impact the oxidation capacity of the troposphere. Acetone, acetaldehyde and MEK are oxidised to peroxy radicals that react with NO_2 to form peroxyacetyl nitrate (PAN), which is an important precursor of tropospheric ozone (Millet et al., 2010; Fischer et al., 2012; Khan et al., 2015; Wang et al., 2019) and can lead to the transport of radicals and NO_2 over long distances. Production of radicals (e.g., OH, HO_x) and PAN further affect the chemistry of the tropospheric ozone (Volkamer et al., 2010; Fischer et al., 2014; Tan et al., 2019, Brewer et al., 2020; Zborowska et al., 2021). Therefore, accurate OVOC monitoring is crucial to assess tropospheric ozone burdens, trends and variability.

The Tropospheric Ozone Assessment Report – Phase I (TOAR-I) identified uncertainties associated to ozone precursors' emissions, including VOCs, as one of the main contributors to the uncertainty of modelled spatial and temporal distribution of ozone (Young et al., 2018). Long-term accurate measurements of ozone precursors are required to reduce the uncertainties of their emissions. This need of accurate measurements was also highlighted in TOAR-I as part of the scientific tasks, goals and requirements for tropospheric ozone monitoring (Tarasick et al., 2019). Other programs and infrastructures for atmospheric monitoring emphasises the importance of monitoring VOCs, particularly OVOCs, because of their active role and impact on chemistry of the atmosphere, air quality and climate change. The World Meteorological Organisation Global Atmosphere Watch (WMO-GAW) programme has listed methanol, ethanol, acetone and formaldehyde as part of reactive gas compounds to be monitored (Schultz et al., 2015). The European Aerosol, Clouds and Trace Gases Research Infrastructure (ACTRIS) (Laj et al., 2024) – through its Centre for Reactive Trace Gases In Situ Measurements (CiGas) – includes OVOCs as one of the four compound clusters to be monitored, together with non-methane hydrocarbons, condensable vapours and NO_x (Hoerger et al., 2015; Simon et al., 2023). Metrological traceability of the measurements, ideally to the International System of Units (SI), is essential to guarantee data comparability among the different monitoring networks (Güttler and Richter, 2009; Brewer et al., 2018; Worton et al., 2023).

Metrological traceability is achieved through an unbroken chain of calibrations, each contributing to the uncertainty of measurements (De Bièvre and Taylor, 1997). One way of ensuring SI-traceability is to calibrate analytical instruments, which are used to monitor atmospheric compounds, against a primary reference material produced by a National Metrology Institute (NMI). NMIs prepare these materials following reference procedures, provide complete uncertainty budgets of the assigned values, ensure their stability period, and participate in international comparisons with other NMIs to achieve SI-traceability (Brewer et al., 2018). However, for certain reactive compounds, such as many OVOCs (e.g., methanol, ethanol), producing reference material is particularly challenging because of surface, non-linearity and matrix effects, as well as because of stability issues and the low amount of substance fractions (at nmol mol^{-1} level) required (Grenfell et al., 2010; Leuenberger et al., 2015; Rhoderick et al., 2019; Persijn and Baldan, 2023).

SI-traceable reference gas mixtures (RGMs) have been developed at NMIs for an increasing number of OVOCs in the last decade (e.g., Brown et al., 2013; Worton et al., 2023). Nevertheless, RGMs are only available at higher amount of substance

fractions than atmospheric ones (Rhoderick et al., 2019; Worton et al., 2022). When monitoring atmospheric OVOCs, these higher amount fractions imply that RGMs must be diluted at monitoring stations before calibrating the analytical instruments. Depending on the dilution procedure, SI-traceability might be lost because of inadequate dilutions (e.g., using dilution devices such as thermal mass flow controllers, whose calibration is not SI-traceable). Another issue faced by OVOC monitoring

105   stations regarding these RGMs is that the matrix gas of the mixture is not the same as ambient air. Quite often, nitrogen is used as matrix gas to ensure the inertness of OVOCs like acetaldehyde. The use of dry nitrogen instead of humidified synthetic air may influence the calibration results. The lack of SI-traceability and long-term stability of OVOC RGMs produced at low amount fraction levels are other limitations that often have negative effects particularly on long-term OVOC measurements. All these aspects have an impact on data comparability and thus on OVOC trend identification.

110   Here we present the efforts done between the metrological and atmospheric monitoring communities to transfer SI-traceability to the field. For that purpose, protocols to produce two types of SI-traceable working standards – based on dynamic dilution of RGMs with dry nitrogen and on certified spiked whole air samples – of selected OVOCs were developed and assessed. OVOCs were selected in close collaboration with stakeholders (e.g., WMO-GAW, ACTRIS) based on their relevance for atmospheric and climate research, on their role as tropospheric ozone precursors and on the lack of accurate, stable and SI-

115   traceable calibration standards. The selected OVOCs were acetaldehyde, acetone, ethanol, methacrolein, methanol, methyl ethyl ketone (MEK) and methyl vinyl ketone (MVK). The amount of substance fractions of the produced working standards were as close as technically feasible to the ambient air amount of substance fractions (< 10 nmol mol^{-1}). In this work, we used the quantity amount of substance fraction (a.k.a. amount fraction) – the metrological accepted term (Richter, 2007; Matschat et al., 2023) – instead of concentration and/or mixing ratio. We expressed this quantity in SI units of nmol mol^{-1}, which can be

120   considered equivalent to part per billion (ppb) under tropospheric conditions (Galbally et al., 2013).

2 Traceable working standards based on dynamic dilution of reference gas mixtures

The first type of SI-traceable working standards developed was based on the dilution of SI-traceable RGMs containing the selected OVOCs at amount fractions slightly higher than in the atmosphere (ca. 100 nmol mol^{-1}). However, the target amount fraction of the SI-traceable working standards was 10 nmol mol^{-1} or lower. Thereby, RGMs were diluted using two dilution

125   systems, both calibrated against national primary standards. Dry nitrogen of high purity (≥ 99.99990 %) was used as matrix and dilution gas to prevent any possible reaction (e.g., oxidation) of OVOCs. The potential presence of water and OVOCs in the matrix and the dilution gas was assessed following standard procedures (ISO 19229:2019, 2019).

2.1 SI-traceable reference gas mixtures

2.1.1 Gravimetric preparation

130   Four RGMs of OVOCs in dry, high-purity nitrogen (BIP+ Built-in-Purifier, Air Products Inc., PA, USA) were prepared at VSL, the National Metrology Institute of the Netherlands, in August 2021. For that purpose, the primary gravimetric method

was used by means of a high-resolution mass comparator (ISO 6142-1:2015, 2015). Known amounts of pure liquid OVOCs were injected in high-pressure gas cylinders to obtain binary gas mixtures at around 50–100 µmol mol⁻¹ in a first step. The injected OVOCs were acetaldehyde (Acros Organics™, PA, USA; purity 99.9 %), acetone (Sigma-Aldrich, MA, USA; purity ≥ 99.99 %), ethanol (Merck KGaA; Germany; purity ≥ 99.99 %), methacrolein (MACR; Thermo Fisher Scientific Inc., PA, USA; 98.5 %), methanol (Sigma-Aldrich®, MO, USA; purity 99.99 %), methyl ethyl ketone (MEK; Acros Organics™, PA, USA; purity 99.9 %) and methyl vinyl ketone (MVK; Acros Organics™, PA, USA; purity 97 %). Prior to the injection, the purity of the liquid OVOCs was analysed (ISO 19229:2019, 2019) using a gas chromatographic (GC) system (6890, Agilent Technologies Inc., CA, USA) with a mass spectrometer (MS) and a flame ionization detector (FID). A GS-GASPRO capillary column (60 m length, 0.32 mm internal diameter and 0.25 µm film thickness; Agilent Technologies Inc., CA, USA) was used for these measurements. For acetaldehyde, it was not possible to perform the purity analysis because of the physical properties of the liquid chemical, which made its handling difficult. The water content in the liquid OVOCs was determined by the Karl Fischer titration (Coulometric KF titrator, Metrohm).

Besides the selected OVOCs, n-hexane (Merck KGaA, Germany; purity ≥ 99.0 %) was injected as internal standard to assess RGM stability. Then, the binary gas mixtures were combined and further diluted to obtain OVOC RGMs at nominal amount fractions around 100 nmol mol⁻¹ and at a pressure of 12 MPa. The RGMs were prepared in 10 L aluminium cylinders (Luxfer Inc., CA, USA) with an Experis® proprietary treatment (Air Products Inc., PA, USA) and a low dead-volume stainless steel cylinder valve D304 (Rotarex, Luxemburg).

2.1.2 Amount fraction assignment and verification

RGM amount fraction value assignment was based on gravimetry, with exception of methanol and ethanol. For these compounds, the value was assigned by analysis against dynamically prepared OVOC RGMs. Metrological traceability of the gravimetric RGMs was ensured by mass weighing and purity determination, while for methanol and ethanol, by mass weighing, volume and purity determination.

After preparation (between end of August and mid-September 2021), RGMs were verified against OVOC gas mixtures that contained acetone, ethanol, methacrolein, methanol, MVK and MEK and were generated by a diffusion method (ISO 6145-8:2005, 2005). Other dynamic preparation methods: continuous syringe injection (ISO 6145-4:2004, 2004) and dynamic dilution of a RGM at high amount fraction (ISO 6145-7:2018, 2018) were used for acetaldehyde. The verification process was repeated three times using VSL thermal desorption (TD)-GC-FID described in Appendix A. The RGMs were connected to an autosampler built by VSL, sharing therefore the same pressure reducer. Lines and pressure reducer were coated (SilcoNert® 2000). To guarantee the same sampling conditions (20 mL min⁻¹ sampling flow during 15 minutes, total volume 300 mL at 293 K and 101.3 kPa) for gravimetric and dynamically prepared RGMs, the mass flow controller (MFC) of the thermal desorber was operated in light vacuum mode by means of a pump. Each gas mixture was analysed 20 times. For each compound, a response factor was calculated according to Eq. (1), which was used to estimate the compound amount fraction in the

gravimetric RGM following Eq. (2). RGM verification was based on the evaluation of the relative difference between the calculated amount fraction and the gravimetric value.

$$RF_i = \frac{(\bar{A}_{cal\_i} - \bar{A}_{0i})}{x_{cal\_i}} \tag{1}$$

where,

RF_i: compound i response factor

$\bar{A}_{cal\_i}$: average peak area of compound i in the calibration standard (last five replicates)

$\bar{A}_{0i}$: average peak area of compound i in the blanks (last five replicates)

x_{cal_i}: amount fraction of compound i in the calibration standard

$$x_i = \frac{(\bar{A}_i - \bar{A}_{0i})}{RF_i} \tag{2}$$

where,

x_i: estimated amount fraction of compound i in the sample

$\bar{A}_i$: average peak area of compound i in the RGM (last five replicates)

$\bar{A}_{0i}$: average peak area of compound i in the blanks (last five replicates)

RF_i: response factor of compound i calculated according to Eq. (1)

Four additional analyses were performed 5 months, 7 months, 13 months and 18 months after preparation to assess the long-term stability of the RGMs. In each period, two to three series of measurements were performed. Relative differences between averaged measured values for each period and gravimetric values were used as an indicator of temporal stability. Furthermore, a comparison between three laboratories took place to complete the RGM amount fraction verification. During this interlaboratory comparison (Appendix B.4), one of the verified VSL RGMs (VSL221418) was analysed at VSL and at the NMIs of France (LNE) and Switzerland (METAS) between January and April 2022 using the analytical methods described in Table B4.

2.1.3 Uncertainty of the RGMs

Preparation and verification uncertainty sources were considered to estimate the uncertainty of the RGMs based on the measurement model proposed in ISO 6142-1:2015 (2015). Regarding the preparation sources, uncertainties from weighing, molar masses and the purity of the materials used was propagated using the law of uncertainty propagation (JCGM 100:2008, 2008). The uncertainty was evaluated using an in-house made software based on the work described in Alink and Van Der Veen (2000). Uncertainty sources linked to RGM verification included the repeatability of each series of measurements and the spread among the series of measurements. A Student's t-test was used to determine whether the mean difference between

average analytical observed values and gravimetric values was significant. When significant, the uncertainty of the recovery due to initial loss was included in the uncertainty evaluation (Eq. (3)).

$$u_c = \frac{1}{2} \cdot \sqrt{u^2(prep) + u^2(ver) + u^2(rec)} \qquad (3)$$

where,

200   u_c: combined uncertainty of the amount fraction of the compound

    u(prep): gravimetric preparation standard uncertainty

    u(ver): analytical verification standard uncertainty

    u(rec): standard uncertainty of the recovery due to initial loss

An additional term was added to the combined uncertainty of the RGMs sent around for SI-working standard assessment

205 (VSL221420 and VSL221421) to account for potential temporal instabilities during the shipment period. The expanded uncertainty was then calculated as the combined uncertainty multiplied by the coverage factor ($k = 2$).

2.2 Dilution systems

Working standards containing OVOCs at atmospheric amount fractions were prepared by diluting the described RGMs with

210 clean and dry nitrogen using two different dilution systems. The first dilution system was developed by VSL and consisted of one-stage gas dilution with dilution flows ranging 2–50 L min⁻¹, allowing dilution ratios up to 1:1000. Flows of the RGM (0.1 L min⁻¹) and of the dilution gas (nitrogen, AP BIP Plus grade 6.0) were accurately controlled using three MFCs (EL-FLOW® Select series, Bronkhorst, Netherlands), operating up to 10 L min⁻¹ and 25 L min⁻¹. The dilution system was mostly built in inert glass. Other materials in contact with the OVOC gas mixtures were PTFE, 316 SS (small surfaces) or coated 316 SS

215 (SilcoNert® 2000, SilcoTek, PA, USA). A coated (SilcoNert® 2000) pressure regulator was connected to the RGMs and flushed thoroughly before attaching it to the dilution system. For the purpose of this assessment, the MFCs were set and calibrated using two mercury piston prover volumeters (Bronkhorst, Netherlands), which were in turn calibrated at the VSL Flow Department, at working ranges of 0–0.5 L min⁻¹ and 0–10 L min⁻¹. Temperature and pressure were measured by equipment calibrated at the VSL Temperature and Pressure Department to convert flow to standard temperature and pressure

220 (STP) conditions (293.15 K, 101.3 kPa).

The second dilution system – referred to as "VeRDi" (Versatile Reactive Gas Diluter) and developed by METAS – was transferred to the institutes assessing the SI-traceable working standards except to VSL. The main components of this two-stage gas dilution system were four MFCs (two MFCs up to 0.1 L min⁻¹ (Red-y, Vögtlin Instruments, GmbH, Switzerland) and two MFCs up to 5 L min⁻¹ (Sensirion AG, Switzerland)), two pressure controllers (Bronkhorst High-Tech B.V.,

225 Netherlands), a valve terminal (MPA-L, Festo Beteiligungen GmbH & Co. KG, Germany) and a vacuum pump. Elements in contact with RGM flow were coated (SilcoNert® 2000), including all the stainless steel tubing of ¼" internal diameter used to build VeRDi. The tubes were welded, instead of joined through fittings, in order to reduce dead volumes and potential leaks.

MFCs and pressure regulators were calibrated using clean and dry nitrogen against METAS primary standards to ensure traceability of the dilution. The software controlling VeRDi was developed in LabVIEW (National Instruments, Austin, TX).

230 Both dilution systems were warmed up for at least 24 hours and flushed with zero gas (i.e., dry high-purity nitrogen) to prevent presence of water or any other contaminant, before the preparation of working standards.

3 Traceable working standards based on certified spiked whole air samples

The second type of SI-traceable working standards developed consisted on certified whole air samples that were previously spiked with the selected OVOCs to obtain amount fractions around 10 nmol mol⁻¹.

235 3.1 Air sampling and vessel filling

Two 50 L aluminium cylinders (parent cylinders) were selected to be filled with ambient air by the Swiss Federal Laboratories for Materials Science and Technology (Empa). Before filling them, the parent cylinders were spiked with water to passivate their inner walls with a layer of water to reduce adsorption and surface reactions of the compounds of interest. First, both cylinders were evacuated in parallel for one hour (cylinder pressure < 10 hPa) with a membrane pump. Then, 0.73 mL of

240 deionized water (Merck Millipore, Germany) was injected individually in each parent cylinder at Empa on 31 March 2021. OVOC spiking was done using a high-pressure cylinder containing an SI-traceable RGM of OVOCs in dry high-pure nitrogen (VSL, Netherlands) at amount fraction levels between 500 nmol mol⁻¹ and 1000 nmol mol⁻¹ (Table C1). The OVOC spiking was performed by connecting the parent cylinders to the SI-traceable RGM via a ¼" cross connector (Swagelok Co., OH, USA) and a vacuum pump fitted with an on/off valve to isolate the pump from the cylinders. The spiking took place at Empa

245 on 21 April 2021. Both, water and OVOC spiking were carried out at room temperature.

After the spiking, the two parent cylinders were filled with ambient air at the National Air Pollution Monitoring Network (NABEL) station at "Rigi Seebodenalp" (ca. 1000 m above sea level; Switzerland) on 22 April 2021. The filling was done using a modified diving compressor (RIX Industries, SA-6). The compressor air inlet was about 2 m above ground and placed upwind of the compressor. Both cylinders were filled in parallel during three hours to a final pressure of ca. 145 bar. After the

250 sampling and once back in the laboratory, the parent cylinders were stored tilted (ca. 30° inclination) over night with the top facing downward. Then, the two parent cylinders were taken outdoors and stored for another hour at ambient temperature (10 °C) vertically upside down, before the valves were opened to release the liquid water that was potentially formed during the filling. Since each the spiking and air filling took place with the two parent cylinders connected in parallel, it was assumed that OVOC amount fractions in both cylinders were identical (Table C1).

255 Six cylinders and 24 canisters (Table C2) were selected for decanting the parent cylinders to produce several identical subsamples (i.e., working standards). Prior to decanting, the working standard cylinders and canisters were spiked with water – following the same procedure described for the parent cylinders – to achieve a 20 % water saturation level. The parent and working standard cylinders, as well as the canisters, were placed in a climate chamber at 40 °C for at least three hours to ensure

thermal equilibration before decanting. The interconnecting tubing was kept as short as possible and several tanks of the same

260 type were filled simultaneously. After decanting the parent cylinders, the absolute pressure ranges in the working standard cylinders and canisters were 9.9–10.5 MPa and 0.38–0.41 MPa, respectively.

3.2 Certification of the spiked whole air samples

The homogeneity of the spiked air samples was evaluated before certification. For that purpose, seven whole air samples in different vessel types and the two parent cylinders after decantation were analysed using Empa GC-FID described in Appendix

265 A. The obtained amount fractions were averaged and the variations within the same vessel type and among different vessel types were calculated. Furthermore, during the certification process, the temporal stability of the whole air samples in cylinders was assessed after 2 months, 8 months and 14 months. Variations due to temporal instability were included in the certified values.

Certification measurements were carried out by VSL and METAS using the two analytical methods described in Table C3

270 and following the same measurement protocol (Appendix C). Each whole air sample was analysed at least six times. In total, three series of measurements for whole air samples in cylinders were performed, but only one measurement series for the samples in canisters was possible due to the limited sample volume. The amount fraction of each compound per whole air sample was calculated according to Eq. (2). The uncertainty of the assigned amount fraction values included the main uncertainty sources of the sample analysis – such as spread of the analyser response, background noise, blank issues, potential

275 overlapping of GC peaks and detector drift among others – and the uncertainty of the analyser calibration (i.e., uncertainty of the RGMs and possible lack of linearity in the measured range: 0–10 nmol mol^{-1}) (Appendix C). The consistency of the assigned amount fraction values for acetone, ethanol, methacrolein, methanol and MVK measured in the same type of vessel was evaluated according to the criterion described by Eq. (4).

$$|x_{VSL} - x_{METAS}| \leq k \cdot \sqrt{u_{VSL}^2 + u_{METAS}^2} \qquad (4)$$

280 where,

x_{VSL}: amount fraction value of each OVOC under study assigned by VSL

x_{METAS}: amount fraction value of each OVOC under study assigned by METAS

k: coverage factor ($k = 2$)

u_{VSL}: standard uncertainty of the amount fraction value assigned by VSL according to Eq. (C1)

285 u_{METAS}: standard uncertainty of the amount fraction value assigned by METAS according to Eq. (C1)

Certified reference values for each type of vessel were assigned only when the criterion (Eq. (4)) was met for all OVOCs in the same type of vessel. In this case, the certified reference value of each OVOC was the average of VSL and METAS assigned values for that compound. The relative uncertainty of the certified reference values was the combined uncertainty of the

290 assigned values provided by VSL and METAS, including the spread of the assigned values due to potential temporal instability (one year period).

4 Assessment of the SI-traceable working standards

4.1 Measurement procedure

The SI-traceable working standards were assessed by comparing them against in-house working standards, which were used
295   for routine calibrations by the participants in the assessment. For that purpose, the selected analysers (Table A1) were calibrated
using the in-house working standards (Appendix D.1) at different amount fraction levels between March and November 2022.
The SI-traceable working standards were treated as samples and analysed following the same procedure as for the analyser
calibration. The detailed analytical method, calibration standards and measurement procedure to assess both types of SI-
traceable working standards are described in Appendix D.

300   The assessment of working standards based on the dilution of RGMs with dry nitrogen (Table 1) was performed by the
Institute Mines-Télécom (IMT), VSL, Utrecht University (UU) and Empa. The measurement sequence consisted of the
measurement of dry pure nitrogen samples to estimate the blank of the system, followed by the measurement of samples
prepared by dynamic dilution of RGMs, which were analysed among the in-house standards.

To assess the SI-working standards based on certified spiked whole air samples, the same air sample cylinders were measured
305   by the participants in the round-robin comparison: Deutscher Wetterdienst (DWD), IMT, VSL, UU and Empa. However,
different canisters were sent to the participants because of the low sample volume, which was enough only for one analysis
(Table C2). After some blank measurements, in-house working standards were assessed at a minimum of two amount fraction
levels between 1 nmol mol^{-1} and 16 nmol mol^{-1}. Samples were measured between in-house working standards. After the second
calibration amount fraction level, blank measurements were performed again.

310   **Table 1: Information on the assessment of working standard (WS) based on dilution of RGMs with dry nitrogen. ECN refers to the effective carbon number.**

Participant	Dates	Samples (assessed WS)	In-house WS[*]	Analytical method
IMT	Jun. 2022	RGM VSL221421 + VeRDi	NPL PTR-MS standard	PTR-ToF-MS
VSL	Aug. 2022	RGM VSL221419 + VSL dilutor	VSL diffusion standard	TD-GC-FID
UU	Sep.-Oct. 2022	RGM VSL221421 + VeRDi	NPL PTR-MS standard	PTR-ToF-MS
Empa	Nov. 2022	RGM VSL221420 + VeRDi	NPL NMHC standard + ECN	TD-GC-FID

[*]All the in-house working standards were SI-traceable except for the effective carbon number (ECN)

4.2 Working standard amount fractions and uncertainty

315   #### 4.2.1 Measured amount fractions and uncertainties

The measured amount fractions of the SI-traceable working standards were calculated using different equations depending on
the analytical method and the calibration standard used.

VSL estimated the amount fractions of the SI-traceable working standards based on the dilution of RGMs with dry nitrogen according to Eq. (2), using only the last five measurements for the calculations. Uncertainty of these measured amount fractions was calculated following Eq. (B1).

320

Empa used the effective carbon number (ECN; e.g., Sternberg et al., 1962; Apel et al., 1998; Faiola et al., 2012) to estimate the OVOC amount fractions from the calibration using an NPL NMHC standard (Grenfell et al., 2010) as the in-house standard. The ECN was the only in-house standard used in this assessment that was not SI-traceable. The uncertainty of the estimated amount fraction was the combination of the standard deviation of the multiple measurements of the sample, the mean relative

325 deviation of the NPL NMHC standard certified uncertainties of the six compounds (ethane, ethene, propane, propene, isobutane and butane) contributing to the CRF and the relative standard deviation of the six calculated CRFs. Uncertainty sources linked to the uncertainty of the instrument (sampling line artefacts, carry over and changes of split flow rates) were considered in the standard deviation of the multiple calibration measurements.

IMT estimated the amount fractions of the selected OVOCs according to the calibration approach described in de Gouw and

330 Warneke (2007) (Appendix D.4). The combined measurement uncertainty, $u(x_i)$, was calculated as the square root of the sum of quadrats of each relative uncertainty term. Sources of uncertainty associated to the measured amount fractions included precision of the system and calibration accuracy (Appendix D.4).

UU followed the method described in Holzinger et al. (2019) to estimate the OVOC amount fractions. The uncertainty of the measured amount fractions was given as the standard deviation of 4–6 repetitions of the same measurement type.

335

4.2.2 Assigned amount fractions and uncertainty

For the SI-traceable working standards based on the dilution of RGMs with dry nitrogen, the assigned amount fraction of each sample was estimated according to Eq. (5).

$$x_{th} = \frac{\left(x_{RGM} \cdot q_{v\_RGM} + x_{res} \cdot q_{v\_dil}\right)}{\left(q_{v\_RGM} + q_{v\_dil}\right)} \qquad (5)$$

340 where,

x_{th}: assigned amount fraction of the generated SI-traceable working standard (in nmol mol^{-1})

x_{RGM}: amount fraction of the OVOC under study in the diluted VSL RGM (in nmol mol^{-1})

x_{res}: amount fraction of the OVOC under study present as residual in the dilution gas (in nmol mol^{-1})

q_{v_RGM}: flow rate of VSL RGM (in mL min^{-1})

345 q_{v_dil}: flow rate of the dilution gas (in mL min^{-1})

The uncertainty of the assigned values was calculated following the law of uncertainty propagation (JCGM 100:2008, 2008) according to Eq. (6). Calculations were done using GUM Workbench Pro version 2.4.1.406 (Metrodata GmbH, Germany).

$$u(x_{th}) = \sqrt{[c_1 \cdot u(x_{RGM})]^2 + [c_2 \cdot u(q_{v\_RGM})]^2 + [c_3 \cdot u(x_{res})]^2 + [c_4 \cdot u(q_{v\_dil})]^2} \qquad (6)$$

where,

$u(x_{th})$: uncertainty of the assigned amount fraction of the generated SI-traceable working standard

$u(x_{RGM})$: uncertainty of the VSL RGM used in the comparison (provided in the calibration certificate according to Eq. (3))

$u(q_{v\_RGM})$: uncertainty of VSL RGM flow rate

$u(q_{v\_dil})$: uncertainty of the dilution gas flow rate

$u(x_{res})$: uncertainty due to the presence of the compound under study in the dilution and matrix gas as impurity

c_1: sensitivity coefficient given by the partial derivative of x_{th} respect x_{RGM}

c_2: sensitivity coefficient given by the partial derivative of x_{th} respect q_{v_RGM}

c_3: sensitivity coefficient given by the partial derivative of x_{th} respect x_{res}

c_4: sensitivity coefficient given by the partial derivative of x_{th} respect q_{v_dil}

Assigned amount fractions and uncertainty of the workings standards based on certified spiked whole air samples were estimated following the procedure described for the air sample certification (Appendix C).

4.2.3 Relative differences between working standards

The assessment of the SI-traceable working standards based on the dilution of RGMs with dry nitrogen was done by calculating the relative difference between the measured and assigned amount fractions described above. The expanded uncertainty of each assessment was calculated as two times the combined uncertainty (u_{diff}) between the uncertainty of the theoretical amount fraction ($u(x_{th})$) and the uncertainty of the measured amount fraction $u(x_i)$ reported by the participants for each compound (Eq. (7).

$$u_{diff} = \sqrt{u^2(x_{th}) + u^2(x_i)} \qquad (7)$$

Measured amount fractions of the SI-traceable working standards based on air samples were compared against the certified OVOC amount fraction values provided by VSL and METAS.

5 Results

5.1 RGM amount fraction assignment and verification

RGM amount fractions were assigned gravimetrically taking into consideration the purity of the liquid chemicals injected into the cylinders and results from the mass weighing during the preparation. Results showed purity values > 99.9 % for all the liquid compounds, except for methacrolein (98.5 %) and MVK (94.0 %). Water was a common impurity in all the liquid compounds. For methacrolein, MVK and MEK, other organic impurities were found (Table B1). Values of the assigned gravimetric amount fractions ranged between 98 nmol mol^{-1} and 105 nmol mol^{-1} with expanded uncertainties of the preparation ≤ 5 % (coverage factor $k = 2$) in general (Table 2). However, greater uncertainties were calculated for methanol (5.3 % in VSL221419 and 6.8 % in VSL221420), acetaldehyde (9.6 % in VSL221420 and 9.5 % in VSL221421) and MVK (5.8 % in VSL221421) to take into account initial losses and potential instability of these compounds in the cylinders.

Table 2: Gravimetric assigned amount fraction values (x_i) for the reference gas mixtures (RGMs) and their expanded uncertainty (U) with a coverage factor of two ($k = 2$)

RGM code	$x_i \pm U$ (nmol mol^{-1})						
	acetaldehyde	acetone	ethanol	methacrolein	methanol	MEK	MVK
VSL221418	103.1 ± 2.6	98.1 ± 1.6	98.0 ± 2.4	100.7 ± 1.6	98.0 ± 3.4	100.2 ± 1.8	101.8 ± 3.0
VSL221419	101.9 ± 2.1	99.3 ± 2.2	99.2 ± 3.2	99.6 ± 2.5	99.2 ± 5.3	99.1 ± 2.5	100.7 ± 4.3
VSL221420	103.3 ± 9.6	97.9 ± 4.4	93.3 ± 3.8	101.0 ± 4.2	99.8 ± 6.8	100.4 ± 3.9	102.1 ± 3.6
VSL221421	101.2 ± 9.5	99.9 ± 3.6	96.6 ± 5.0	99.0 ± 4.1	105.1 ± 5.0	98.4 ± 3.4	100.0 ± 5.8

Results from the verification analysis (Table B2), where the prepared RGMs were compared against dynamically generated gas mixtures, showed similar relative differences between analytical and gravimetric values for acetone in the four cylinders (average difference < +0.54 %). These results, similar to the relative differences found for the internal standard (n-hexane), suggest that surface effects (i.e., adsorption losses) were negligible for both compounds. For MEK, the analytical values were also greater than the gravimetric ones and quite similar among different cylinders (average difference < +3.2 %). Lower analytical values than gravimetric ones were found for acetaldehyde, methacrolein and MVK. Average differences were < +2 % and similar among different cylinders for acetaldehyde and methacrolein, which suggests minimal or even negligible adsorption effects with the cylinder wall. The difference was higher for MVK (between -2.5 % and 3.7 %), which might be explained not only by surface effects but also by isomerization reactions. All the relative differences were within the expanded uncertainty of the verification analysis. Compound loss after preparation due to surface effects might explain relative differences of around -5 % for ethanol. Initial losses were also suggested by the great heterogeneity among cylinders for methanol (relative difference between -5.2 % and +3.1 %) like described in Persijn and Baldan (2023).

Long-term stability results (Table B3) suggested very good stability (i.e., relative differences between analytical and gravimetric values smaller than ± 5 %) for acetone with relative differences ≤ +2 % even 13–14 months after RGM preparation,

although a questionable result (-4.7 %) was obtained at a stability testing period of 18–19 months. Acetone results were similar to those for the internal standard (n-hexane). A good stability was also found for methacrolein. After initial relative differences of ca. -1.5 %, positive values around +0.7 % were found 7–8 months after preparation. The positive values increased up to

405   3.4–3.7 % during the last stability period (18–19 months). MVK and MEK showed respectively fluctuating positive (up to +5.7 %) and negative (up to -6.4 %) relative differences most likely due to analytical issues, isomerization reactions and/or surface effects. Ethanol showed a negative relative difference which remained within the ± 5 % threshold, except for one of the measurement results obtained at months 18–19 (-5.1 %). Acetaldehyde and methanol long-term stability had the largest biases. Varying relative differences > ± 5 % (positive for acetaldehyde and negative for methanol) were already found after 5–

410   6 months after preparation, which could be explained by analytical issues, matrix effects and initial compound losses due to adsorption effects.

During the interlaboratory comparison organized as part of the RGM verification process (Appendix B.4), the three participant laboratories (VSL, METAS and LNE) measured acetone, ethanol and methanol. Results demonstrated a very good comparability and degree of equivalence for acetone (Fig. 1). For methanol, a good agreement among laboratories was also

415   found (Fig. B1), as well as for ethanol. However, due to the great expanded uncertainty (37 %) of the ethanol measurement associated to METAS analytical issues, these results were not considered. It can be noted that although different calibration and analytical methods were used, the measurement results of the RGMS were aligned giving confidence on the quality of the work.
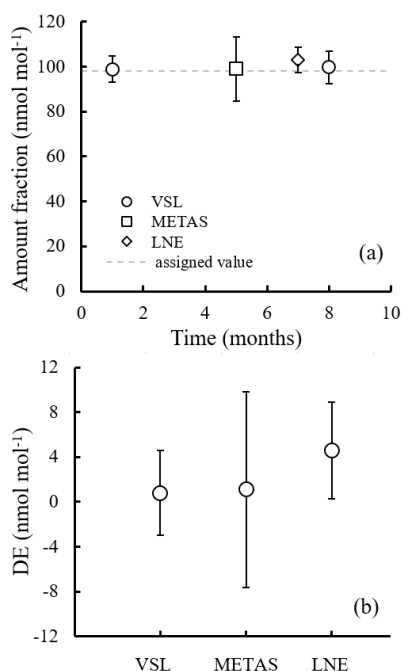
420   **Figure 1: Interlaboratory comparison results for (a) acetone and (b) its degree of equivalence (DE; i.e., the deviation of each laboratory from the reference value). For VSL, only the first measurement period was considered (month 1) to estimate the DE. The measured amount fractions reported by the laboratories were the average of 5 measurements, except for month 1 results, which**

were the average of 3 measurements. Error bars show the expanded uncertainty of the measurements (coverage factor k = 2). The dashed line indicates the gravimetric amount fraction of the compound.

425

5.2 Certified amount fractions of the spiked whole air samples

Results showed good homogeneity (variation < 5 %) within the same vessel type for all selected OVOCs. The greatest variation was found for methanol (+3.2 %). For the rest of OVOCs, the variation was ≤ +1.5 % (e.g., +0.6 % for acetone, +0.9 % for MVK, +1.2 % for MEK and +1.5 % for acetaldehyde and ethanol). Variation among different vessel types suggested that the vessel material may play a role in the lack of homogeneity particularly for methanol (+22.6 %) and ethanol (+9.7 %). Variation was relatively great also for acetaldehyde (+6.6 %), MEK (+6.6 %) and MVK (+7.0 %). However, good homogeneity was found for acetone (+2.8 %) and toluene (+2.4 %). Although toluene is not an OVOC and, thus, was not spiked into the whole air sample vessels, the compound was naturally present in the ambient air.

Temporal stability of the air samples was evaluated by Empa considering the ratio between each OVOC and the internal standard (i.e., n-hexane). Acetone to n-hexane ratios showed good temporal stability (i.e., differences in ratio values among measurements within the uncertainty of the measurement) during the measuring period from August 2021 to September 2022. Except for the uncertainties that were greater, similar results were found for other compounds (methanol, ethanol, acetaldehyde, MVK and MEK). Because the ratio differences observed were within the uncertainty of the measurements and the homogeneity among vessels of the same type was good (variation < +2 % except for methanol (+3.2 %)), air samples in the same type of vessel were considered stable.

Certification results obtained for whole air samples contained in pressurised 10 L aluminium cylinders showed good consistency between the two laboratories performing the certification (i.e., VSL, METAS), with exception of MVK (criterion was not met (Eq. (4)). Regarding the other type of pressurised cylinders (3.6 L stainless steel SilcoNert® coated), the criterion was neither met for MVK. For methanol, the criterion was met only when METAS results were compared against the results obtained for the first measurements performed by VSL (i.e., July 2021). Certified OVOC amount fractions in both cylinders (Table 3) ranged between 7.6 nmol mol^{-1} (ethanol) and 17.3 nmol mol^{-1} (acetone) with expanded uncertainties (k = 2) ≤ 2.6 nmol mol^{-1} (Table 3). The smallest uncertainties were found for methacrolein and acetone (≤ 1.5 nmol mol^{-1}). Amount fractions were in line with the estimated spiked values (Table C1) suggesting that, except for acetone, the amount fractions of the selected OVOCs in the sampled air were not significant (close to zero). The higher amount fractions measured for acetone compared to the spiked estimated amount fractions suggested acetone background levels in the sampled whole air of around 6.5 nmol mol^{-1}.

Results of the low-pressure canisters were less consistent: the criterion was only met for methacrolein for four canisters (Table C4). For methanol and acetone, the criterion was only met in two canisters. The discrepancy between results for the 15 L canister suggested homogeneity issues for this batch.

455

Table 3: Certified amount fraction values (x) and their expanded uncertainty (U; coverage factor $k = 2$) estimated for the air samples filled in the high-pressure cylinders: 10 L cylinder (MVOC151-001) and 3.6 L (MVOC151-002).

compound	$x_{MVOC151\text{-}001} \pm U$ [nmol mol^{-1}]	$x_{MVOC151\text{-}002} \pm U$ [nmol mol^{-1}]
methanol	12.8 ± 2.0	$9.8 \pm 2.5^{*}$
ethanol	11.2 ± 2.6	7.6 ± 1.9
acetone	17.0 ± 1.5	17.3 ± 1.1
methacrolein	10.7 ± 1.0	10.2 ± 0.9
MVK	$9.4 \pm 2.6^{*}$	$8.4 \pm 2.3^{*}$
MEK	$12.3 \pm 2.3^{**}$	$12.1 \pm 2.4^{**}$

*no compliance with evaluation criterion described in Eq. (4)

460 **measurement carried out by only one of the laboratories

5.3 Assessment of SI-traceable working standards based on dilution of RGMs

The assessment of the SI-traceable working standards based on the dilution of RGMs with dry nitrogen took place during a long period of time (ca. six months between the first and last participants). Potential temporal instabilities were considered

465 when comparing results through the certified expanded uncertainty provided with the RGMs (Table 2). The long-term RGM stability of each compound was evaluated and taken into account as an uncertainty term (Table B3). The type of in-house standard, sampling method and analytical instrument used, as well as the amount fraction level of the samples generated, were most likely the parameters explaining the differences found between VSL and the other participants for certain compounds, such as MEK (Fig. 2) and methanol (Fig. 3).

470 Despite relative differences around ±20 % for IMT and Empa, a good agreement between assigned and analytical values (i.e., relative difference around 0 considering the uncertainty of the difference) was found for acetone, even at amount fractions < 5 nmol mol^{-1} (Fig. 2). This agreement demonstrated the reliability of the dilution systems, RGMs and calibration methods. The great relative differences obtained by Empa for acetone were explained by technical issues with the analytical method (i.e., a leak in the heated valve and flow overshooting when measuring with the Stirling cooling unit). The error was estimated

475 to be around ± 30 % and was included in the uncertainty budget. These issues also affected Empa MEK and methanol measurements. Therefore, care should be taken in the interpretation of these results.

Similar results to acetone working standards were obtained for MEK at amount fractions around 10 nmol mol^{-1} (Fig. 2). At lower amount fraction levels (< 5 nmol mol^{-1}), some of the measurements showed analytical fraction values lower than the assigned ones.

480 Methanol relative differences were relatively small (1–14 %) and within the uncertainty range at amount fractions between 10 nmol mol^{-1} and 17 nmol mol^{-1} (Fig. 3). However, at lower amount fractions (< 5 nmol mol^{-1}) relative differences were

between 25–65 %, which suggest an overestimation of the analytical amount fraction values most likely due to artefacts in the analytical system. Moreover, the temporal instability of methanol within the gas cylinder, with an increase in the amount fraction observed during the first year after preparation for one of the RGMs, might contribute to explain the overestimation.

485 Methanol instability in gas cylinders was observed in other works (Rhoderick et al., 2019; Persijn and Baldan, 2023). Methanol assessment results suggest, thus, that this OVOC remains a challenging compound to measure.

Acetaldehyde measured and assigned amount fractions showed relatively good agreement, i.e., all the differences were within the uncertainty range (Fig. 4). However, these results must be taken with care because of the large uncertainties. Reactions in the gas cylinders and/or artefacts of the analytical methods might have contributed to analytical amount fractions greater than

490 the theoretical values for acetaldehyde, as well as to uncertainties greater than for the other OVOCs.
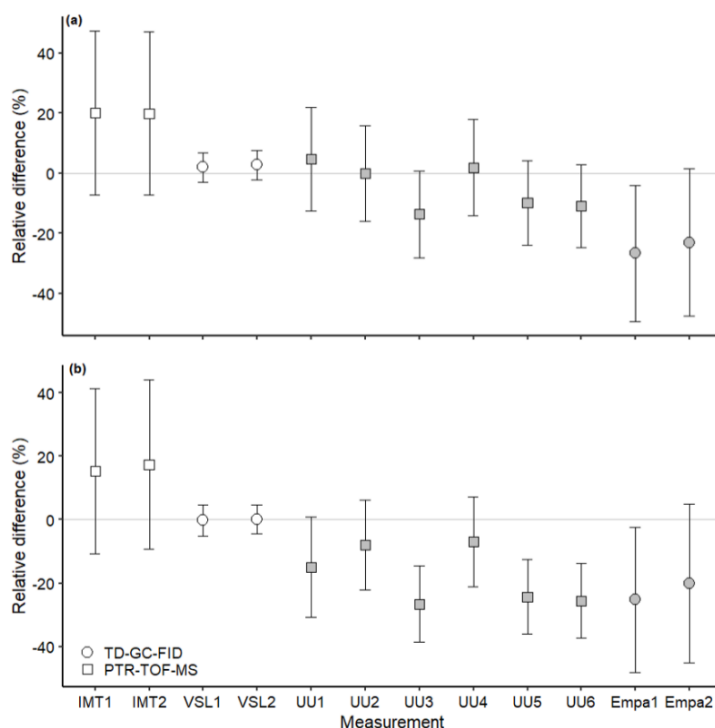
505 **Figure 2: Assessment of the SI-traceable working standards based on the dilution of reference gas mixtures with dry nitrogen for (a) acetone and (b) MEK at amount fractions < 5 nmol mol^{-1} (grey symbols) and between 10–17 nmol mol^{-1} (white symbols). Error bars indicate the expanded uncertainty (coverage factor $k = 2$) of the relative difference between in-house and dilution working standards. Measurement labels show the participant and the number of SI-traceable working standards generated by dilution. Measurements were performed in July 2022 (IMT1, IMT2), August 2022 (VSL1, VSL2), September 2022 (UU1-UU6) and November 510 2022 (Empa1, Empa2).**

515
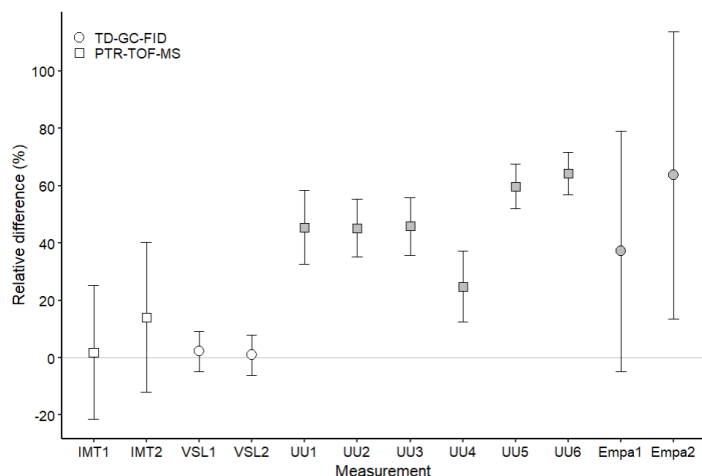
Figure 3: Assessment of the SI-traceable working standards based on the dilution of reference gas mixtures with dry nitrogen for methanol at amount fractions < 5 nmol mol^{-1} (grey symbols) and between 10-17 nmol mol^{-1} (white symbols). Error bars indicate the expanded uncertainty (coverage factor $k = 2$) of the relative difference between in-house and dilution working standards. Measurement labels show the participant and the number of SI-traceable working standards generated by dilution. Measurements were performed in July 2022 (IMT1, IMT2), August 2022 (VSL1, VSL2), September 2022 (UU1-UU6) and November 2022 (Empa1, Empa2).
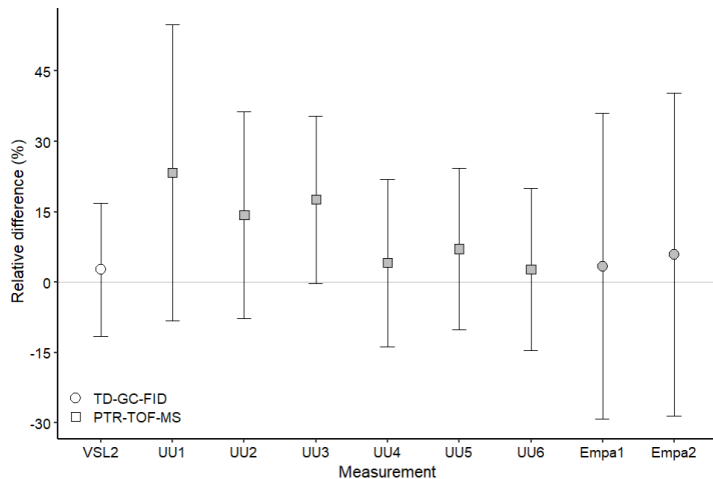
Figure 4: Assessment of the SI-traceable working standards based on the dilution of reference gas mixtures with dry nitrogen for acetaldehyde at amount fractions < 5 nmol mol^{-1} (grey symbols) and between 10-17 nmol mol^{-1} (white symbols). Error bars indicate the expanded uncertainty (coverage factor $k = 2$) of the relative difference between in-house and dilution working standards. Measurement labels show the participant and the number of SI-traceable working standards generated by dilution. Measurements were performed in August 2022 (VSL2), September 2022 (UU1-UU6) and November 2022 (Empa1, Empa2).

Assessment results for amount fraction levels around 10 nmol mol^{-1} suggests that SI-traceable working standards based on dilution of RGMs can be used as calibration standard at monitoring stations for key OVOCs, such as acetone. For other OVOCs, like methanol, acetaldehyde and MEK, suitability is not so clear due to the large uncertainty and result dispersion,

particularly at amount fractions < 5 nmol mol⁻¹. The different analytical methods used, the calibration procedure followed and the dilution factors applied to measure and prepare the SI-traceable working standards contributed to that. Further research following the same calibration procedure (e.g., same in-house working standard) and assessment protocol (e.g., setting the

555 same dilution factors to generate SI-traceable working standards at the same amount fractions) may reduce both uncertainty and dispersion and help to draw conclusions. Moreover, using coated (e.g., SilcoNert 2000) lines – as short as possible – and low-dead volume pressure regulators, as well as performing long enough measurements to guarantee the stability of analyser and dilutor, may reduce the uncertainty of the generated working standards. Even if results are not conclusive, the low RGM uncertainty (< 5 %) and long temporal stability (at least up to 15 months after preparation) are promising to provide atmospheric

560 monitoring stations with SI-traceable accurate OVOC working standards at very low amount fractions.

5.4 Assessment of SI-traceable working standards based on certified spiked whole air samples

Amount fractions of the OVOCs measured in air samples showed good agreement (Fig. 5, Fig. 6) among partners. These values

565 were comparable to the certified amount fractions for whole air samples in cylinders (pressurised at 9.8–10.5 MPa). Only for methanol (Fig. 6), values were more discrepant. Empa results, as for the SI-traceable working standards based on dilution of RGMs with dry nitrogen, must be interpreted with caution because of the technical issues with the analytical system.
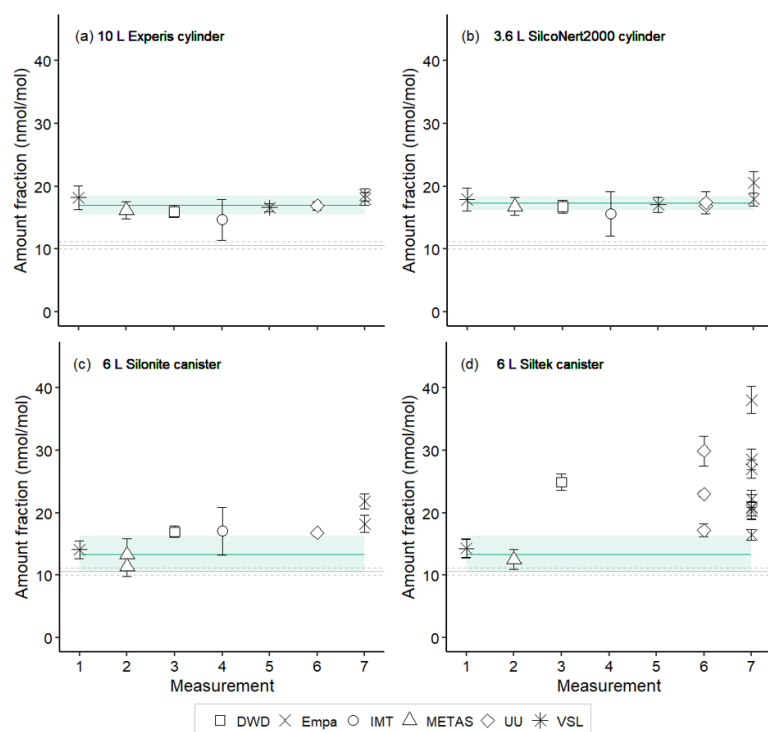
Figure 5: Assessment of the SI-traceable working standards based on certified spiked whole air samples for acetone in (a) 10 L
570 **Experis® aluminium cylinders, (b) 3.6 L SilcoNert® 2000 stainless steel cylinders, (c) 6 L Silonite™ stainless steel canisters and (d)**

6 L Siltek® stainless steel canisters. Spiked amount fraction (solid grey line), certified amount fraction (solid green line) and their expanded uncertainty (dashed lines) are shown. Error bars indicate the expanded uncertainty (coverage factor $k = 2$) of the relative difference between in-house and dilution working standards. Measurements were performed in Jul. 2021 (1), Feb. 2022 (2), Mar. 2022 (3), Jun. 2022 (4), Aug. 2022 (5), Sep. 2022 (6) and Nov. 2022 (7).

575   For whole air samples in canisters (pressurised at 0.35 MPa), results were quite heterogeneous. Relatively good results were found for acetone (Fig. 6) and MEK in the Silonite™ stainless steel canisters. However, for methanol and acetaldehyde, disagreement was found both among most of the participants and with the certified values. Lack of agreement was also observed for air samples in the Siltek® stainless steel canisters. Even if the same cleaning procedure was followed by both type of canisters before filling, the history (i.e., previous fillings) of the Siltek® stainless steel canisters and/or the surface

580   treatment could explain the differences between canister types. History and surface treatments effects on VOC amount fractions have been reported in previous works (e.g., Rhoderick et al., 2019; Persijn and Baldan, 2023). Furthermore, vessel pressure might explain the differences in result agreement between cylinders and canisters. Gas pressure effects on the stability of gas mixtures in cylinders have been observed for different compounds, such as CO_2 (e.g., Leuenberger et al., 2015; Miller et al., 2015). In these studies, after an initial wall adsorption when the cylinders were filled, desorption took place. This

585   adsorption-desorption process resulted in increasing amount fractions. In Silonite™ canisters, the treatment might have contributed to a lower initial wall adsorption compared to the Siltek® canisters and, therefore, to the lower discrepancies.
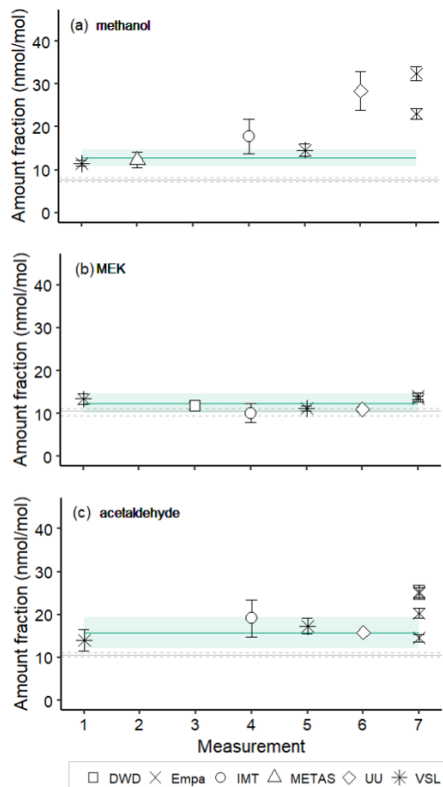
Figure 6: Assessment of the SI-traceable working standards based on certified spiked whole air samples in 10 L Experis® aluminium cylinders for (a) methanol, (b) methyl ethyl ketone (MEK) and (c) acetaldehyde. Spiked amount fraction (solid grey line), certified

amount fraction (solid green line) and their expanded uncertainty (dashed lines) are shown. Error bars indicate the expanded uncertainty (coverage factor $k = 2$) of the relative difference between in-house and dilution working standards. Measurements were performed in Jul. 2021 (1), Feb. 2022 (2), Mar. 2022 (3), Jun. 2022 (4), Aug. 2022 (5), Sep. 2022 (6) and Nov. 2022 (7).

Assessment results suggest that certified spiked whole air samples at low amount fractions (< 20 nmol mol^{-1}) in compressed gas cylinders may be used as SI-traceable working standards for most of the selected OVOCs, except for methanol, at monitoring stations. Using the same matrix gas as the ambient air monitored at atmospheric stations may improve the accuracy of the observations by reducing artefacts and other effects related to the matrix gas.

6 Conclusions

VOCs are one of the major tropospheric ozone precursors. Despite the importance of performing accurate and comparable VOC measurements to assess tropospheric ozone trends, several challenges regarding VOC monitoring remain currently open. For example, the lack of stable and SI-traceable gas reference materials for many OVOCs at ambient levels and adapted to constraints of monitoring stations (e.g., limited dilution gas supply) among others. This research has shown that producing SI-traceable RGMs at amount fractions around 100 nmol mol^{-1}, with expanded uncertainties of the preparation < 5 % and temporal stability of at least 14 months, is doable for acetone, methacrolein, MEK, MVK and, to some extent, for ethanol. However, further research is needed to find suitable cylinder materials and optimal preparation and analytical procedures to minimize surface adsorption and reaction effects, which greatly contributed to the temporal instability of RGMs for methanol and acetaldehyde.

Besides RGMs, SI-traceable working standards at lower amount fractions (i.e., ambient levels; 4–10 nmol mol^{-1}) to calibrate VOC analyzers at monitoring stations are needed to ensure comparability of the VOC measurements within and among monitoring networks. Here, we presented the developed and assessed protocols to generate two different types of SI-traceable working standards. The first type, based on RGMs diluted with dry nitrogen, using for that a portable dilution system that ensures SI-traceability after dilution, seems to be suitable for calibration of acetone, MEK and methanol at amount fractions around 10 nmol mol^{-1}. The second type, based on certified spiked whole air samples filled into high-pressure cylinders might become also a valid alternative for calibrating instruments measuring acetone, acetaldehyde and MEK at monitoring stations. Despite these promising findings, conclusions must be driven with caution because of the large values and the broad range obtained for the measurement uncertainties (i.e., 5–31 %; coverage factor $k = 2$). For both types of working standards, methanol calibration remains challenging.

The RGMs and working standards described in this work are a first step to fulfil the remaining needs of VOC monitoring. Through an active collaboration among metrological, meteorological and atmospheric chemistry monitoring communities, harmonization and comparability among monitoring stations will be promoted (e.g., by estimating uncertainty budgets that are common to the different monitoring programs). Moreover, this collaboration might provide a better understanding of the impact that pressure, sampling material, moisture and matrix have on the preparation of RGMs and working standards. This

knowledge may contribute, thus, to improve calibration standards (i.e., RGMs and SI-traceable working standards) and uncertainties of VOC measurements. Furthermore, other research applications, such as modelling and remote sensing, might

625 benefit from the transfer of SI-traceability to monitoring stations.

Appendix A: Analytical instruments

Thermal Desorption-Gas Chromatography-Flame Ionization Detector (TD-GC-FID) and Proton Transfer Reaction-Time of Flight-Mass Spectrometry (PTR-ToF-MS) were the two selected analytical methods in this work. The specific analytical instruments used by the laboratories are summarised in Table A1.

630 **DWD**

DWD deployed a GC-FID/MS system (6890, 7590 inert XL MS, Agilent Technologies Inc., CA, USA), which was coupled to a custom-made sample pre-concentration unit that included sampling valves, sampling ports and the preconcentration trap in a box heated to 150 °C. Materials in the sampling path were mainly treated stainless steel or capillaries. Samples were preconcentrated on multibed sorbent tubes (Tenax TA 60/80 mesh, Carbopack X 40/60 mesh and Carboxen 695 20/45 mesh

635 in a ¼" glass tube, Merck KGaA (Supelco), MO, USA) at 30 °C with a sampling flow of 80 mL min^{-1}. Desorption to a cryo-focus trap (inert capillary cooled to -180 °C) took place at 200 °C with a flow of 10 mL min^{-1}. After heating the cryo-focus to 60 °C, the sample was injected splitless onto a BPX-5 capillary column (50 m length, 0.32 mm internal diameter, 0.5 µm film thickness, Trajan Scientific and Medical (SGE), Australia). The GC oven was held at 13 °C for 18 min. Then, the oven temperature was increased up to 240 °C at a rate of 6 °C min^{-1}. Hydrogen (H$_2$ 5.0 from Air Liquide, France) cleaned using a

640 gas filter (Super Clean gas filter, Restek, PA, USA) was used as a carrier gas at 3.5 mL min^{-1}. Subsequent to the separation on the column, the carrier gas flow was split onto the MS and the FID in parallel.

Empa

Empa used a GC-FID (7890, Agilent Technologies Inc., CA, USA) coupled to a thermal desorber UNITY™-xr (Markes International Ltd., UK) to evaluate the stability and homogeneity of the air samples and to assess the SI-traceable OVOC

645 working standards (Table A1). Samples went through an in-house dehumidifier – consisting of a Stirling cooler (set to -42 °C) and two insulated in-line glass fingers – before sampling, which was done using a UNITY™-Air Server (Markes International Ltd., UK) equipped with three ports. From UNITY™-Air server, samples passed to the thermal desorber, which collected and concentrated the OVOCs under study. The UNITY cold trap (ozone precursors cold trap, U-T17O3P-S2; Markes International Ltd., UK) temperature was set to -29 °C before the cold trap was heated up to 250 °C. The two capillary columns were

650 OxyPLOT (30 m length, 0.53 mm internal diameter and 10 µm film thickness; Agilent Technologies Inc., CA, USA) and Al$_2$O$_3$ HP-PLOT (50 m length, 0.53 mm internal diameter and 10 µm film thickness; Agilent Technologies Inc., CA, USA). Sample flow was set at 15 mL min^{-1} during 20 min. The GC oven was held at 40 °C for 3.25 min and then heated up to 200 °C with a temperature ramp of 7 °C min^{-1}. The GC oven was held at 200 °C for 20 min. The carrier gas was helium, which was set at 5 mL min^{-1} for 20 min and then increased at 25 mL min^{-1} for 26 min.

IMT

655 IMT performed the assessment of SI-traceable working standards using a second generation PTR-ToF-MS (Kore Technology Ltd., UK) (Table A1). Sampling was done through a SilcoNert® 1000 heated line at a flow rate of 200 mL min⁻¹. An in-house system of solenoid valves was coupled to the PTR-ToF-MS to switch automatically between samples and zero air. Measurement time resolution was set to 10 seconds.

LNE

660 LNE used a GC-FID (7890, Agilent Technologies Inc., CA, USA), equipped with an on-column pre-concentration system, during the OVOC RGM comparison (Table A1). The selected capillary column was HP-Plot-U (30 m length, 0.53 mm internal diameter and 20 µm film thickness; Agilent Technologies Inc., CA, USA). The GC oven was held at a constant temperature of 150 °C. The carrier was helium BIP® (Air Products and Chemicals, PA, USA). The sampling was done using a coated

665 (SilcoNert® 2000) sample loop, which injected a sample volume of 60 mL. The pre-concentration system was cooled down to -60 °C by a liquid nitrogen cryo trap system (JAS 66601 CryoTrap, Joint Analytical Systems GmbH, Germany), which was heated up to 150 °C for final injection.

METAS

METAS used a GC-FID Clarus 500 (PerkinElmer Inc., MA, USA) coupled to a thermal desorber TurboMatrix 350

670 (PerkinElmer Inc., MA, USA) (Table A1). The capillary column was DuraBond DB-624 (30 m length, 0.32 mm internal diameter and 1.8 µm film thickness; Agilent Technologies Inc., CA, USA). The carrier was helium. The system had a Tenax-TA sorbent cold trap (Perkin Elmer Inc., MA, USA), which was cooled at -30 °C and heated up to 280 °C at a temperature rate of 40 °C s⁻¹. The GC oven was held at 40 °C for 2 min and then heated up to 200 °C at 5 °C min⁻¹. The GC oven was held at 200 °C for 2 min. The sampling was done using conditions multibed sorbent tubes: Carbograph 2TD (mesh 60/80) –

675 Carbograph 1TD (mesh 40/60) – Carbosieve™ SIII (mesh 60/80) (Camsco, TX, USA). Loading of the sorbent tubes were done by means of an in-house loading system at loading volumes between 300 mL (10 min at 30 mL min⁻¹) and 450 mL (15 min at 30 mL min⁻¹).

UU

UU used a PTR-ToF-MS with hexapole and ion funnel (PTR-TOF4000, Ionicon Analytik GmbH, Austria) to assess the SI-

680 traceable working standards (Table A1). A SulfiNert® coated 4-port valve (VICI® Valco Instruments Co. Inc., TX, USA) kept at 120 °C was used to switch between zero air and sample inlet. Samples were connected to a PEEK capillary that, depending on the pressure in cylinders and canisters, produced a flow between 80 mL min⁻¹ and 300 mL min⁻¹.

VSL

VSL used TRACE™ GC (Thermo Fisher Scientific Inc., PA, USA) coupled to a thermal desorber UNITY™ 2 (Markes

685 International Ltd., UK) during the OVOC comparison, the certification of air samples and the assessment of SI-traceable working standards (Table A1). A Deans switch in the GC sent the gas sample to two FID detectors and two capillary columns: Stabilwax (30 m length, 0.32 mm internal diameter and 1.0 µm film thickness; Restek Corporation, PA, USA) for MVK and PoraBOND U (25 m length, 0.32 mm internal diameter and 7 µm film thickness; Agilent Technologies Inc., CA, USA) for the

other OVOCs. The cold trap filled with multi-bed sorbent trap (Air Toxics, Markes International Ltd., UK) was cooled down

690   to -20 °C and heated up to 300 °C. Sampling flow was set at 20 mL min^{-1} during 30 min. The GC oven was held at 40 °C for

2 min and then heated up to 230 °C with three temperature ramps of 20 °C min^{-1} (up to 120 °C), 5 °C min^{-1} (up to 180 °C) and

10 °C min^{-1} (up to 230 °C). The GC oven was held at 200 °C for 20 min. The carrier gas was helium.

Table A1: Information on the analytical instruments used in this work.

Lab	Measurements	Analytical method	Analytical instrument
DWD	Assessment[2]	TD-GC-FID/MS	6890 GC-FID (Agilent), 7590 inter XL MS (Agilent) Custom made TD unit (DWD)
Empa	Assessment[1,2]	TD-GC-FID	7890 GC-FID (Agilent) TD UNITY™-xr (Markes International)
IMT	Assessment[1,2]	PTR-ToF-MS	second-generation PTR-ToF-MS (Kore Technology)
LNE	Comparison	TD-GC-FID	7890 GC-FID (Agilent)
METAS	Comparison, certification	TD-GC-FID	Clarus 500 GC-FID (Perkin Elmer) TD TurboMatrix 350 (Perkin Elmer)
UU	Assessment[1,2]	PTR-ToF-MS	PTR-TOF4000 (Ionicon Analytik)
VSL	Comparison, certification, assessment[1,2]	TD-GC-FID	Thermo Trace GC-FID; TD UNITY™ 2 (Markes International)

695   [1]Assessment SI-traceable working standards based on dilution of RGMs with dry nitrogen

[2]Assessment SI-traceable working standards based on certified spiked whole air samples

Appendix B: Purity analysis, stability evaluation and verification of the RGMs

B.1 Purity analysis

700   The liquid OVOCs used to prepare the gravimetric RGMs were analysed to determine their purity (Table B1).

Table B1: Purity of the liquid OVOCs used to prepare the gravimetric reference gas mixtures including the amount fraction of compounds and impurities (x_i) and its expanded uncertainty ($U(x_i)$; coverage factor k = 2). CAS refers to the chemical abstract service registry number. The purity analysis of acetaldehyde (CAS 75-07-0) was not possible because of handling difficulties associated to the physical properties of the liquid chemical.

Liquid chemical	CAS	Compound	x_i (mol mol^{-1})	$U(x_i)$ (mol mol^{-1})
Acetone	67-64-1	acetone	0.999380	0.000124
		water	0.000620	0.000124
Ethanol	64-17-5	ethanol	0.999733	0.000054
		water	0.000267	0.000054
Methacrolein	78-85-3	methacrolein	0.985646	0.001683
		methylal	0.003458	0.000692
		1,1-dimethoxy-2-butene	0.003600	0.000720
		hydroquinone	0.001000	0.000500
		water	0.006296	0.001260
Methanol	67-56-1	methanol	0.999724	0.000056
		water	0.000276	0.000056
Methyl Ethyl Ketone (MEK)	78-93-3	MEK	0.999297	0.000147
		2,4-dimethyl-hexane[2]	0.000234	0.000118
		trichlorodocosyl-silane[3]	0.000037	0:000019
		water	0.000431	0.000087
Methyl Vinyl Ketone (MVK)	78-94-4	MVK	0.940938	0.005352
		Acetonitrile	0.008389	0:001678
		4-(acetyloxy)-2-butanone	0.006077	0.001216
		2-acetyl-5-methyl-2,3-dihydro-4H-pyran[1]	0.020687	0.002069
		p-benzoquinone	0.001564	0.000313
		water	0.022346	0.004470
n-Hexane	110-54-3	n-hexane	0.991224	0.001307
		3-methyl-pentane	0.002943	0:000589
		methyl-cyclopentane	0.005831	0:001167
		water	0.000002	0.000001

705   [1]The impurity might also be MVK dimer.

[2]According to MS database, the first hit with highest probability is 2,4-dimethyl-hexane, but the probability is only around 10 %.

[3]According to MS database, the first hit with highest probability is trichlorodocosyl-silane, but the probability is only around 15 %.

B.2 RGM stability evaluation

710   Results of the long-term stability evaluation for two of the prepared RGMs (VSL221418 and VSL221419) are shown in Table B3. The evaluation was carried out immediately after preparation (0–1 month). Other stability periods considered were 5–6 months, 7–8 months, 13–14 months and 18–19 months after preparation of the RGMs.

Table B3: Temporal stability of two of the gravimetric RGMs. Results are expressed as relative difference (Δ) of the average analytical value with respect to the gravimetric value. Deviations larger than ± 5 % are in bold. The stability period is indicated as the number of months after RGM preparation. NA indicates not available data due to an analytical issue during a measurement.

RGMs	Stability period (months)	$\Delta_{acetaldehyde}$ (%)	$\Delta_{acetone}$ (%)	$\Delta_{ethanol}$ (%)	$\Delta_{methacrolein}$ (%)	$\Delta_{methanol}$ (%)	Δ_{MEK} (%)	Δ_{MVK} (%)	$\Delta_{n\text{-hexane}}$ (%)
VSL221418	0–1	-2.2	0.9	-1.8	-1.3	1.8	3.3	-2.7	0.8
	5–6	NA	NA	NA	NA	NA	NA	NA	NA
	7–8	**9.6**	1.2	-3.5	0.7	**-7.1**	4.9	-3.6	0.9
	13–14	**16.1**	1.9	-2.6	3.7	**-8.4**	0.1	**-6.4**	1.8
	18-19	**5.8**	0.2	-1.4	3.4	-4.5	-0.1	-0.6	0.5
VSL221419	0–1	-0.6	0.6	-2.0	-1.4	0.2	3.1	-3.3	0.3
	5–6	**-7.1**	0.4	-2.5	0.9	**7.6**	**5.7**	-4.4	-0.6
	7–8	**8.3**	0.9	-0.2	0.7	**7.1**	4.6	-4.4	0.3
	13–14	**14.7**	1.5	0.1	3.2	**5.9**	-0.1	**-6.2**	1.2
	18-19	**5.7**	-4.7	**-5.1**	3.7	-2.5	0.2	-0.7	-4.7

B.3 RGM verification

B.3.1 Verification measurement results

Results of the verification measurements performed one month after preparation of the RGMs are shown in Table B2. Three verification measurements were carried out for each RGM.

Table B2: Verification results obtained one month after preparation of the RGMs gravimetrically prepared RGMs at VSL. Three verification measurements (M1, M2 and M3) of the amount fraction of each compound (x_i) were performed per RGM. The relative standard deviation (RSD) and the relative difference between analytical and gravimetric values (Δ) are also shown. NA indicates not available data due to an analytical issue during a measurement.

Compound	RGM code	x_{i_M1} (nmol mol^{-1})	x_{i_M2} (nmol mol^{-1})	x_{i_M3} (nmol mol^{-1})	RSD (%)	Δ (%)
acetaldehyde	VSL221418	101	102	99.2	1.40	-2.24
	VSL221419	NA	101	102	1.61	-1.48
	VSL221420	99.0	102	102	1.78	-2.22
	VSL221421	95.5	97.6	106	5.68	-1.47
acetone	VSL221418	98.7	99.4	98.9	0.37	0.90
	VSL221419	NA	98.9	101	1.03	0.41
	VSL221420	98.4	97.4	99.5	1.10	0.53
	VSL221421	100	101	99.7	0.53	0.33
ethanol	VSL221418	97.6	95.8	95.5	1.19	-1.75

Compound	RGM code	X_{i_M1} (nmol mol^{-1})	X_{i_M2} (nmol mol^{-1})	X_{i_M3} (nmol mol^{-1})	RSD (%)	Δ (%)
	VSL221419	NA	95.7	98.7	5.90	-5.12
	VSL221420	93.3	91.0	93.8	1.57	-5.26
	VSL221421	96.6	97.8	90.8	3.93	-4.75
methacrolein	VSL221418	98.9	99.8	99.6	0.48	-1.29
	VSL221419	NA	97.0	99.4	1.23	-1.62
	VSL221420	99.2	98.4	101	1.29	-1.47
	VSL221421	97.0	97.7	99.1	1.08	-1.05
methanol	VSL221418	103	98.8	97.6	2.77	1.78
	VSL221419	NA	96.7	102	10.2	-5.21
	VSL221420	93.5	98.1	101	4.08	-0.14
	VSL221421	106	105	98.2	4.00	3.11
MEK	VSL221418	103	104	103	0.64	3.29
	VSL221419	NA	101	103	0.80	2.91
	VSL221420	103	103	104	0.78	3.07
	VSL221421	101	102	102	0.42	3.21
MVK	VSL221418	99.0	99.2	99.1	0.11	-2.66
	VSL221419	NA	96.3	98.5	1.40	-3.71
	VSL221420	99.0	97.4	99.1	0.99	-3.50
	VSL221421	95.6	97.7	99.3	1.93	-2.48

725

B.3.2 RGM interlaboratory comparison

LNE, METAS and VSL took part in an interlaboratory comparison to verify the produced RGMs. Three different TD-GC-FID systems and calibration methods (Table B4) were used to analyse the amount fraction of acetone, ethanol and methanol in the RGM sent around (VSL221418).

730   The same coated (SilcoNert® 2000) pressure reducer (RX 2400, Rotarex, Luxemburg) and line (1/16" coated line of 1 m length) were used, for at least one series measurements, by LNE and METAS. VSL used an autosampler (VSL spin) equipped with a multi-position valve (VICI AG International, Switzerland), a coated (SilcoNert® 2000) pressure regulator (Tescom, TX, USA) and coated lines (SilcoNert® 2000, 1/16" diameter, ca. 1 m length). Five series of measurements were performed by LNE and by METAS. VSL performed three series of measurements before shipping the comparison standard to the other

735 laboratories (September 2021) and five series of measurements after the shipment (April 2022). At least five replicates per series were analysed. Individual measurement sequences consisted in the analysis of blank samples (at the beginning and end of each measurement), calibration standard samples (at two amount fraction levels) and comparison standard samples, which were (analysed between the calibration standards to minimise drift effects and prevent biases. LNE sampling was done through

a coated (SilcoNert® 2000) sample loop of 20 mL volume; total sample volume was 60 mL. VSL sampling was done by means

740 of the autosampler (Unity 2, Markes International, Ltd., UK) coupled to the TD-GC-FID at a sampling flow rate of 20 mL

min^{-1} during 15 minutes (300 mL sample volume). Multibed sorbent tubes (Carbograph 2 (mesh 60/80) – Carbograph 1 (mesh

40/60) – Carbosieve™ SIII (mesh 60/80); Camsco, TX, USA) were used for sampling by METAS; loading volume ranged

between 150 mL and 450 mL.

Amount fraction values of the comparison standard were assigned applying Eq. (1) and Eq. (2). Following standard

745 procedures used in key comparisons, the degree of equivalence of each laboratory for acetone was estimated as the difference

between analytical measurement values obtained by each laboratory and the gravimetric reference value provided by VSL.

Table B4: Information on the interlaboratory comparison measurements of one of the OVOC reference gas mixtures (RGMs; VSL221418) prepared by VSL to generate SI-traceable working standards based on its dilution using dry nitrogen.

Lab	Date	Analytical instrument	Capillary column (length, internal diameter, film thickness)	Calibration method
LNE	March 2022	Agilent 7890 GC-FID	Agilent HP-Plot-U (30 m, 0.53 mm, 20 µm)	Dynamic dilution (ISO 6145-7:2018)
METAS	January 2022	Perkin Elmer Clarus 500 GC-FID; thermal desorber TurboMatrix 350	Agilent DuraBond DB-624 (30 m, 0.32 mm, 1.8 µm)	Permeation (ISO 6145-10:2002)
VSL	September 2021, April 2022	Thermo Trace GC-FID; Markes International thermal desorber Unity 2	Agilent PoraBond U (25 m, 0.32 mm, 7 µm)	Diffusion (ISO 6145-8:2005)

750
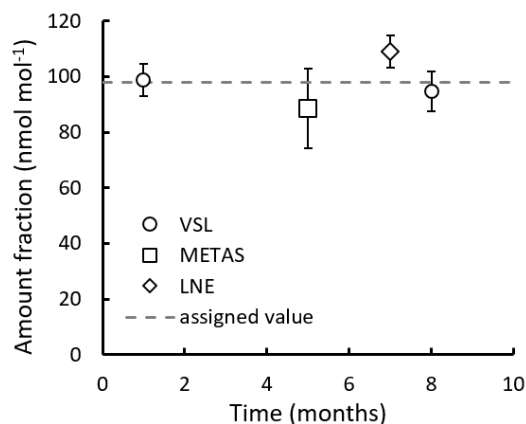
Figure B1: Interlaboratory comparison results for methanol. Reported values were the average of 5 measurements, except for month 1 results, which were the average of 3 measurements. Error bars show the expanded uncertainty of the measurements (coverage
755 **factor k = 2). The dashed line indicates the gravimetric amount fraction of the compound.**

Appendix C: Whole air sample spiking and certification

To spike the two parent cylinders with the selected OVOCs, a certified RGM filled into a high-pressure 5 L aluminium cylinder (D249650, VSL, Netherlands) was used. The RGM contained acetaldehyde, acetone, ethanol, methacrolein, methanol, MEK,

760 MVK, benzene, n-hexane and propane in dry nitrogen at amount fractions between 500 and 1004 nmol mol^{-1} (Table C1). The cylinder content was transfer to the parent cylinders through a cross connector joined to the outlet of the RGM cylinder (that was heated to avoid condensation), to the parent cylinders and to the vacuum pump used to evacuate the RGM cylinder. Because dilution factors of around 0.011 were expected after whole air filling of the parent cylinders, the RGM cylinder was fully evacuated into the parent cylinders to reach OVOC spiked values between 5 nmol mol^{-1} and 10 nmol mol^{-1} (Table C1).

765

Table C1: Amount fraction (x_{cyl}) and certified expanded uncertainty ($U(x_{cyl})$) of the OVOCs contained in the gas cylinder used for spiking the air samples. Estimated spiked amount fractions (x_{spiked}) and uncertainties ($U(x_{spiked})$) in the parent cylinders are also included. The coverage factor of the uncertainty is two ($k = 2$).

Compound	x_{cyl}	$U(x_{cyl})$	Dilution	x_{spiked}	$U(x_{spiked})$
	(nmol mol^{-1})	(nmol mol^{-1})	factor (ratio)	(nmol mol^{-1})	(nmol mol^{-1})
acetaldehyde	1000	40	0.011	10.61	0.60
acetone	1001	30	0.011	10.62	0.54
ethanol	866	43	0.011	9.19	0.59
methacrolein	991	30	0.011	10.52	0.53
methanol	721	36	0.011	7.65	0.49
MEK	999	100	0.011	10.60	1.15
MVK	1002	50	0.011	10.63	0.68
benzene	1004	30	0.011	10.66	0.54
n-hexane	500	15	0.011	5.31	0.27
propane	997	30	0.011	10.58	0.53

770

To produce the SI-traceable working standards of certified spiked whole air samples, six cylinders and 24 canisters (Table C2) were filled with the spiked whole air contained in the two parent cylinders. For that purpose, the parent cylinders were decanted into the selected cylinders and canisters to produce several identical subsamples (i.e., working standards). Four cylinders were 10 L aluminium cylinders with Experis® treatment for non-methane hydrocarbon (NMHC) VOC (Air Products

775 Inc., PA, USA) and two were 3.6 L coated (SilcoNert® 2000) stainless steel cylinders (Swagelok Co., OH, USA). Twelve of the selected canisters were coated with Silonite™ (ten 6 L stainless steel canisters and two 15 L stainless steel canisters; Entech Instruments, CA, USA) and twelve were coated with Silcosteel® (6 L stainless steel; Restek Corporation, PA, USA).

Table C2: Air sample cylinders and canisters used to perform one of the described actions: certification, assessment and/or stability.
780 **Actions performed on the vessels were certification (C), assessment (A) and stability (S).**

Vessel MVOC151-	Tank S/N	Tank wall material	Coating/ Treatment	Tank volume (L)	Tank final pressure ($\cdot 10^3$ hPa)	Action	Participant
001A	APE201891	Aluminium[1]	Experis®	10	105	C	VSL
001B	APE917209	Aluminium[1]	Experis®	10	105	A	EMPA, IMT, UU
001C	APE1047602	Aluminium[1]	Experis®	10	105	C	METAS
001D	APE152484	Aluminium[1]	Experis®	10	105	S	EMPA
002A	UD2034	Stainless steel[2]	SilcoNert® 2000	3.6	98.8	C	VSL, METAS
002B	UU9013	Stainless steel[2]	SilcoNert® 2000	3.6	98.8	A/S	EMPA/EMPA, IMT, UU
003A	2566	Stainless steel[3]	Silonite™	15	4.08	C	VSL, METAS
003B	2565	Stainless steel[3]	Silonite™	15	4.08	A/S	EMPA/EMPA, IMT, UU
004A	12938	Stainless steel[3]	Silonite™	6	3.50	C	METAS
004B	5690	Stainless steel[3]	Silonite™	6	3.50	C	METAS
004C	12200	Stainless steel[3]	Silonite™	6	3.50	A	IMT
004D	11330	Stainless steel[3]	Silonite™	6	3.50	A	UU
004E	12202	Stainless steel[3]	Silonite™	6	3.50	S	EMPA
005A	5358	Stainless steel[3]	Silonite™	6	3.50	S	EMPA
005B	3590	Stainless steel[3]	Silonite™	6	3.50	C	VSL
005C	5685	Stainless steel[3]	Silonite™	6	3.50	C	VSL
005E	12201	Stainless steel[3]	Silonite™	6	3.50	C	METAS
006A	5032	Stainless steel[4]	Siltek®	6	4.09	S	EMPA
006B	5040	Stainless steel[4]	Siltek®	6	4.09	C	METAS
006C	5043	Stainless steel[4]	Siltek®	6	4.09	A	IMT
006D	5033	Stainless steel[4]	Siltek®	6	4.09	C	VSL
007A	5041	Stainless steel[4]	Siltek®	6	4.16	C	METAS
007B	5036	Stainless steel[4]	Siltek®	6	4.16	C	VSL
007C	5045	Stainless steel[4]	Siltek®	6	4.16	A	UU
007D	5038	Stainless steel[4]	Siltek®	6	4.16	S	EMPA
008A	5037	Stainless steel[4]	Siltek®	6	4.08	C	METAS
008C	5030	Stainless steel[4]	Siltek®	6	4.08	S	EMPA
008D	5034	Stainless steel[4]	Siltek®	6	4.08	C	VSL

[1]Air Products, [2]Swagelok, [3]ENTECH Instruments, [4]RESTEK

Certification of the air samples was done using two TD-GC-FID (Table C3) and following the same measurement sequence: blanks, air sample, calibration standard at low amount fraction level (1–24 nmol mol^{-1}, depending on the compound), air
785 sample and calibration standard at high amount fraction level (10–45 nmol mol^{-1}, depending on the compound). VSL

calibration standards consisted of two multi-compound gas mixtures at 2 nmol mol^{-1} and 10 nmol mol^{-1} for acetone, methanol, ethanol, acetaldehyde, methacrolein, methyl vinyl ketone (MVK) and methyl ethyl ketone (MEK) in nitrogen. The calibration standards were prepared by diluting two gravimetric RGMs containing these OVOCs in nitrogen, as well as n-hexane and propane, at 100 nmol mol^{-1} and 1000 nmol mol^{-1}. An additional calibration standard containing acetone, ethanol, methanol and

790   n-hexane in clean and dry air at ca. 10 nmol mol^{-1} was obtained by diffusion. METAS generated calibration standards containing acetaldehyde, acetone, ethanol, methacrolein, methanol and MVK in nitrogen at around 10 nmol mol^{-1} by the permeation method (ISO 6145-10:2002 (ISO, 2002)) using a magnetic suspension balance (Waters, DE, USA) and a portable generator (Pascale et al., 2017).

Table C3: Analytical methods used for the certification of air samples

Lab	Date	Analytical instrument	Capillary column (length, internal diameter, film thickness)	Sampling method
VSL	Jul. 2021	Thermo Trace GC-FID; Markes International thermal desorber Unity 2	Agilent PoraBond U (25 m, 0.32 mm, 7 µm) Restek Stabilwax for MVK (30 m, 0.32 mm, µm)	Autosampler (600 mL sampling volume)
METAS	Feb. 2022	Perkin Elmer Clarus 500 GC-FID; thermal desorber TurboMatrix 350	Agilent DuraBond DB-624 (30 m, 0.32 mm, 1.8 µm)	Carbograph 2 (60/80) – Carbograph 1 (40/60) – Carbosieve™ SIII (60/80) multibed sorbent tubes (300–750 mL loading volume)

795

The uncertainty of the assigned amount fraction of each compound and air sample was the results of multiplying the combined uncertainty of each air sample by the coverage factor (k = 2). The combined uncertainty was estimated as the combination of the uncertainty of the calibration standards, the mean standard deviation of the measurements results and the pooled standard deviation of the measurements (Eq. (B1)).

800   $$u^2(x_{sample}) = x_{sample}^2 \left(\frac{u^2(x_{cal})}{x_{cal}^2} + \frac{u^2(\overline{RF}_{cal})}{\overline{RF}_{cal}^2} + \frac{u^2(\bar{y}_{sample})}{\bar{y}_{sample}^2} + u^2(pooled\_sd) \right) \tag{C1}$$

where,

  $u(x_{sample})$: uncertainty of the assigned amount fraction of the compound in the air sample

  x_{sample}: assigned amount fraction of the compound in the air sample

  $u(x_{cal})$: uncertainty of the amount fraction of the compound in the calibration standard

805   x_{cal}: amount fraction of the compound in the calibration standard

  $u(\overline{RF}_{cal})$: mean standard deviation of the response factor of the compound calibration standard

  $\overline{RF}_{cal}$: average response factor of the compound calibration standard (average of three measurements)

  $u(\bar{y}_{sample})$: mean standard deviation of the GC-FID compound responses (average of three measurements)

$\bar{y}_{sample}$: average GC-FID compound response (average of three measurements)

810 $u(pooled\_sd)$: pooled standard deviation of the measurement results

Table C4: Analytical amount fraction values (x_a) and their expanded uncertainty (U; coverage factor $k = 2$) obtained by the two National Metrology Institutes (NMIs) certifying the air samples: VSL and METAS.

vessel MVOC151-	NMI	date	methanol (nmol mol^{-1})		ethanol (nmol mol^{-1})		acetone (nmol mol^{-1})		methacrolein (nmol mol^{-1})	
			x_a	$U(x_a)$	x_a	$U(x_a)$	x_a	$U(x_a)$	x_a	$U(x_a)$
001A	VSL	07/2021	11.5	0.7	11.1	1.0	18.2	1.9	11.5	0.7
001A	VSL	09/2022	14.6	1.5	10.0	0.5	16.6	0.6	10.0	0.6
001C	METAS	02/2022	12.3	1.8	12.4	6.5	16.2	1.4	10.6	0.9
002A	VSL	07/2021	9.2*	0.5	8.7	0.8	17.9	1.8	11.0	0.7
002A	METAS	02/2022	8.1*	1.3	7.8	3.7	16.8	1.4	10.1	0.9
002A	VSL	09/2022	12.1*	2.0	6.3	0.3	17.1	1.2	9.6	0.6
003A	VSL	07/2021	21.9*	1.8	11.8*	1.1	18.9*	1.9	18.1*	1.0
003A	METAS	02/2022	15.2*	1.4	6.0*	2.7	15.4*	1.5	9.9*	0.9
005B	VSL	07/2021	8.2	0.8	10.1*	0.9	14.1*	1.4	8.5	0.5
005E	METAS	02/2022	8.9	1.5	1.4*	0.8	11.4*	1.6	8.9	1.3
007B	VSL	07/2021	4.2*	0.8	10.2*	0.9	14.3	1.4	8.7	0.5
007A	METAS	02/2022	7.5*	0.9	2.0*	1.1	12.5	1.6	9.3	0.9

*values for which the criterion described in Eq. (4) was not fulfilled

Appendix D: Assessment of the SI-traceable working standards

815 **D.1 In-house working standards**

The analytical instruments selected to assess the SI-traceable working standards (Appendix A; Table A1) were calibrated with in-house working standards generated using different methods.

The TD-GC-FID/MS system used by DWD to assess the working standards based on certified spiked whole air samples was calibrated using one of the RGMs prepared by VSL for this work (OVOCs in nitrogen at 100 nmol mol^{-1}). The RGM was

820 diluted with dry nitrogen to achieve amount fraction levels < 10 nmol mol^{-1}. In addition, DWD TD-GC-FID/MS system was calibrated using a primary reference material containing 30 non-methane hydrocarbons (NMHCs) considered ozone precursors (NPL NMHC standard; Grenfell et al., 2010). NPL NMHC standard was diluted at 1 nmol mol^{-1} amount fraction for the calibration. The same type of standard (NPL NMHC) at 2 nmol mol^{-1} amount fraction was used to calibrate Empa TD-GC-FID.

825   The ion transmission curves of both PTR-ToF-MS were determined using a SI-traceable certified reference material produced
by NPL (NPL PTR-MS standard) (Worton et al., 2023) as in-house working standards. The in-house working standards (NPL
D961410 used by IMT and D961397 used by UU) contained 20 compounds at amount fractions around 1 µmol mol^{-1} covering
a mass spectrum from *m/z* 33 to *m/z* 671. Prior instrument calibration, the in-house working standards were diluted with zero
air (i.e. dry nitrogen) down to amount fractions < 10 nmol mol^{-1}.

830   VSL TD-GC-FID was calibrated using RGMs based on the diffusion method (dynamic preparation method ISO 6145-8) as
in-house working standards for acetone, ethanol, methacrolein, methanol, MEK and MVK. For acetaldehyde, an in-house
working standard was obtained by dynamic dilution of a 1 µmol mol^{-1} multi-component RGM containing acetaldehyde,
acetone, ethanol, methacrolein, methanol, MEK, MVK and propane in nitrogen. Three to six in-house working standards were
prepared in the range 4–20 nmol mol^{-1}.

835

D.2 Measurement procedure for assessing the working standards based on dynamic dilution of RGMs

Samples were prepared by dynamic dilution of RGMs. VSL, IMT and UU generated two samples. VSL set the same dilution
factor for both samples (10 times dilution to obtain OVC amount fractions close to 10 nmol mol^{-1}), while Empa and IMT used
different dilution factors (Table D1). UU prepared six samples using different dilution factors (Table D1).

840   Before performing the measurement sequence, VSL sampled and analysed 15 times the pure nitrogen used for dilution to
clean the analytical system and to assess the system blank. Each in-house standard (three to six in total) and sample (i.e., SI-
traceable working standard) was sampled at a flow rate of 20 mL min^{-1} for 30 minutes.

Empa ran five to ten GC runs with a sample of similar humidity level and composition that the matrix gas to condition the
GC-FID. After the conditioning, six consecutive runs without injecting any sample were measured to estimate the system
845   blank. Then, six in-house working standard runs were followed by six runs for each sample (i.e., SI-traceable working
standard). In-house working standard and blank runs (12 runs in total) were repeated after the last sample measurement.
Sampling volume was set at 300 mL (20 minutes at 15 mL min^{-1}).

IMT measurement sequence started with 30 minutes of zero air sampling to quantify background signals and to verify signal
stability. The zero air was obtained using a catalytic converter containing platinum wool (high sensitivity catalyst for TOC
850   analyser, Shimadzu Corporation, Japan), which was heated up to 350 °C. Blank measurements were performed before and
after each new sample test and calibration. After the first blank measurements, the calibration took place by analysing in-house
working standards during 60–90 minutes. The in-house working standards (5 mL min^{-1}) were diluted with a zero-air flow rate
of 1 L min^{-1}. Flows were regulated by MFCs in a Gas Calibration Unit (GCU, Ionico Analytik GmbH, Austria). Then, each
sample was analysed for 90 minutes. The same sampling line coated with SilcoNert® 1000 and sampling flow rate of 100 mL
855   min^{-1} were used for blanks, calibration standards and samples.

UU measured each sample 2–4 times for at least 30 seconds. Before and after each sample measurement, UU analysed blanks
(i.e., zero air produced by a heated platinum catalyst) and the in-house working standard (NPL-PTR-MS standard). Blanks,

in-house working standards and samples were injected through a sample loop (250 µL volume) according the procedure

described in Holzinger et al. (2019). The in-house working standards (loop flow of 10 mL min^{-1}) were diluted with a zero-air

860 flow of 240 mL min^{-1}. Sample flows, depending on the pressure in cylinders and canisters, were produced between 80 mL

min^{-1} and 300 mL min^{-1}.

D.3 Measurement procedure for assessing working standards based on certified whole air samples

The same air sample cylinders were assessed by the participants (round-robin comparison). However, different canisters were

865 sent to the participants because of the low sample volume, which was enough only for one analysis (Table C2). Participants

followed a similar measurement sequence than the measurement procedure described for the SI-traceable working standards

based on RGM dilution. After some blank measurements (six times for GC-FID and 30 minutes for PTR-ToF-MS), in-house

working standards were measured at minimum two amount fraction levels (six times per level for GC-FID and for PTR-ToF-

MS, IMT measured for 90 min and UU for 1 min). Samples were measured between calibration levels (6 times each sample

870 for GC-FID and 90 minutes per sample for PTR-ToF-MS measurements at IMT and 1 min at UU). Blank measurements were

performed again after the second amount fraction level of the calibration.

Table D1: VeRDi flow rates (in mL min^{-1}) used to dilute VSL SI-traceable RGM during the assessment of SI-traceable working standards by each laboratory. Gas flow rates correspond to the flow rate of VSL SI-traceable RGM (q_{v_RGM}), first-step dilution flow rate (q_{v_d1}), split flow rate (q_{v_sp}) and second-step dilution flow (q_{v_d2}). The relative expanded uncertainties (coverage factor $k = 2$) of
875 **the flow rates are shown between brackets. The amount fractions of the selected compounds are shown together with their expanded uncertainties ($k = 2$), both expressed in nmol mol^{-1}.**

| | q_{v_RGM} | q_{v_d1} | q_{v_sp} | q_{v_d2} | $x_{acetaldehyde}$ | $x_{acetone}$ | $x_{methanol}$ | x_{MEK} | x_{MVK} |
	(±0.4%)	(±0.3%)	(±0.5%)	(±0.3%)	± U	± U	± U	± U	± U
IMT1	100	520	-	-	16.4±1.5	16.12±0.59	16.96±0.81	15.87±0.56	16.13±0.94
IMT2	60	520	-	-	10.56±0.99	10.34±0.38	10.88±0.52	10.18±0.35	10.34±0.61
UU1	45	1455	100	1400	0.30±0.09	0.21±0.02	0.22±0.02	0.20±0.01	0.20±0.02
UU2	90	1400	100	1410	0.49±0.09	0.40±0.02	0.42±0.03	0.38±0.02	0.39±0.03
UU3	12	1488	-	-	0.91±0.11	0.81±0.04	0.85±0.05	0.79±0.03	0.80±0.05
UU4	24	1476	-	-	1.72±0.18	1.61±0.06	1.69±0.09	1.58±0.06	1.60±0.10
UU5	30	1470	-	-	2.12±0.21	2.01±0.08	2.11±0.11	1.97±0.07	2.00±0.12
UU6	60	1440	-	-	4.14±0.39	4.00±0.16	4.21±0.21	3.94±0.14	4.00±0.24
Empa1	14	650	-	-	2.34±0.23	2.14±0.10	2.18±0.15	2.18±0.09	2.22±0.08
Empa2	20	1450	-	-	1.51±0.15	1.35±0.07	1.37±0.10	1.37±0.06	1.40±0.06

D.4 IMT measured amount fractions

IMT estimated the amount fractions of the selected OVOCs according to the calibration approach described in de Gouw and Warneke,(2007) and following Eq. (D1). In practice, a sensitivity factor of H_3O^+ normalized to 10^6 cps ($Sn(RH+)$) is derived for each targeted compound during calibration experiments. This sensitivity factor comprises the parameters: k_{PTR}, Δt, $T(RH^+)$ and $T(H_3O^+)$. The approach used in de Gouw and Warneke (2007) to account for humidity-dependent sensitivities was applied in this work.

$$x_i = \frac{1}{k_{PTR}\cdot\Delta t} \cdot \frac{I(RH^+)}{T(RH^+)} \cdot \left(\frac{I(H_3O^+)}{T(H_3O^+)}\right)^{-1} = \frac{\frac{I(RH^+)}{I(H_3O^+)}\cdot 10^6}{S_N(RH^+)} \tag{D1}$$

where,

x_i: amount fraction of the compound R (i.e., OVOC under study)

k_{PTR}: proton-transfer-reaction rate coefficient of $R + H_3O^+ \rightarrow RH^+ + H_2O$

Δt: reaction time in the drift tube

$I(RH^+)$: observed signal (counts per second, cps) for the protonated ion RH^+

$I(H_3O^+)$: observed signal (cps) for the reagent ion H_3O^+

$T(RH^+)$: transmission efficiency for RH^+

$T(H_3O^+)$: transmission efficiency for H_3O^+

$S_N(RH^+)$: sensitivity factor of H_3O^+ normalized to 10^6 cps.

Sources of uncertainty associated to the measured amount fractions included the precision of the system and the calibration accuracy. The uncertainty linked to the precision of the system (u_{prec}) was calculated according Eq. (D2). The uncertainty associated to the calibration accuracy (u_{cal_acc}) was estimated applying Eq. (D3).

$$u_{prec} = \frac{\sqrt{I_m(RH^+)+I_Z(RH^+)}}{S_N(RH^+)\cdot I(H_3O^+)} \cdot 10^6 \tag{D2}$$

where,

u_{prec}: measurement precision expressed as amount fraction

$I_m(RH^+)$: RH^+ signal (cps) observed when a sample was measured

$I_z(RH^+)$: RH^+ signal (cps) observed when zeroing the instrument

$I(H_3O^+)$: observed signal (cps) for the reagent ion H_3O^+

$S_N(RH^+)$: sensitivity factor of H_3O^+ normalized to 10^6 cps

$$u_{cal\_acc} = \sqrt{\left(\frac{u(x_{cyl})}{x_{cyl}}\right)^2 + \frac{1}{(q_{v\_cal}+q_{v\_dil})^2} \cdot \left(\frac{q_{v\_dil}^2}{q_{v\_cal}^2} \cdot u(q_{v\_cal})^2 + u(q_{v\_dil})^2\right)}$$ (D3)

where,

u_{cal_acc}: relative combined uncertainty of the calibration accuracy

x_{cal}: OVOC amount fraction generated after dilution of the calibration standard

$u(x_{cyl})$: standard uncertainty of the OVOC amount fraction in the calibration standard (calibration certificate)

x_{cyl}: OVOC amount fraction in the calibration standard (calibration certificate)

q_{v_cal}: flow rate of the calibration standard

q_{v_dil}: flow rate of the dilution gas

$u(q_{v\_cal})$: standard uncertainty of the calibration standard flow rate

$u(q_{v\_dil})$: standard uncertainty of the dilution gas flow rate

Data availability

Data will be made available after acceptance in MetClimVOC Zenodo community
(https://zenodo.org/communities/19env06_metclimvoc/about).

Author contribution

SR, PS, CP, MI-G, AB, TS, AC and RH designed the study. AB, JL and SP prepared the reference gas mixtures (RGMs) used for generated SI-traceable working standards based on the dilution of RGMs. PS, MH and MKV prepared the SI-traceable working standards based on air samples, which were certified by AB and MI-G. AA designed and coordinated the development of the VeRDi dilution system, with supervision of CP. For the assessment measurements, ES, SD, TS and RH performed the PTR-ToF-MS measurements and PS, MH, AB and AC performed the TD-GC-FID measurements. AB, JL, CS and MI-G carried out the OVOC RGM comparison. MI-G wrote the paper with assistance from all authors, who provided information on instrument description and data. All authors reviewed and approved the latest version of the paper.

Competing interests

The contact author has declared that none of the author has any competing interests.

Acknowledgments

935 We acknowledge the technical staff at ACTRIS CiGaS units (IMT Nord Europe, Empa, DWD) and the participating laboratories for their support. Special thanks to the Tropospheric Ozone Precursors Focus Working group for their valuable comments to improve the paper. Utrecht University received support from the Ruisdael Observatory, a scientific infrastructure co-financed by the Dutch Research Council (NOW, grant number 184.034.015).

Financial support

940 This research was performed within the framework of the project 19ENV06 MetClimVOC, which has received funding from the EMPIR programme cofinanced by the Participating States and from the European Union's Horizon 2020 research and innovation programme.

References

Alink, A. and Van Der Veen, A. M. H.: Uncertainty calculations for the preparation of primary gas mixtures Part 1: Gravimetry,
945   Metrologia, 37, 641–650, 2000.

Apel, E. C., Calvert, J. G., Greenberg, J. P., Riemer, D., Zika, R., Kleindienst, T. E., Lonneman, W. A., Fung, K., and Fujita, E.: Generation and validation of oxygenated volatile organic carbon standards for the 1995 Southern Oxidants Study Nashville Intensive, Journal of Geophysical Research Atmospheres, 103, 22281–22294, https://doi.org/10.1029/98JD01383, 1998.

950 Atkinson, R.: Atmospheric chemistry of VOCs and NOx, Atmos Environ, 34, 2063–2101, https://doi.org/10.1016/S1352-2310(99)00460-4, 2000.

Bates, K. H., Jacob, D. J., Wang, S., Hornbrook, R. S., Apel, E. C., Kim, M. J., Millet, D. B., Wells, K. C., Chen, X., Brewer, J. F., Ray, E. A., Commane, R., Diskin, G. S., and Wofsy, S. C.: The Global Budget of Atmospheric Methanol: New Constraints on Secondary, Oceanic, and Terrestrial Sources, Journal of Geophysical Research: Atmospheres, 126,
955   https://doi.org/10.1029/2020JD033439, 2021.

De Bièvre, P. and Taylor, P. D. P.: Traceability to the SI of amount-of-substance measurements: From ignoring to realizing, a chemist's view, Metrologia, 34, 67–75, https://doi.org/10.1088/0026-1394/34/1/10, 1997.

Boucher, O., Randall, D., Artaxo, P., Bretherton, C., Feingold, G., Forster, P., Kerminen, V.-M., Kondo, Y., Liao, H., Lohmann, U., Rasch, P., Satheesh, S.K., Sherwood, S., Stevens, B., and Zhang, X. Y.: Clouds and aerosols in *Climate*
960   *Change 2013: The Physical Science Basis. Contribution of Working Group I to the Fifth Assessment Report of the Intergovernmental Panel on Climate Change* (eds Stocker, T.F., Qin, D., Plattner, G.-K., Tignor, M., Allen, S.K.,

Doschung, J., Nauels, A., Xia, Y., Bex, V., and Midgley, P. M.), Cambridge University Press, 571–657, https://doi.org/10.1017/CBO9781107415324.016 (2013).

Brewer, J. F., Fischer, E. V., Commane, R., Wofsy, S. C., Daube, B. C., Apel, E. C., Hills, A. J., Hornbrook, R. S., Barletta,
965   B., Meinardi, S., Blake, D. R., Ray, E. A., and Ravishankara, A. R.: Evidence for an Oceanic Source of Methyl Ethyl Ketone to the Atmosphere, Geophys Res Lett, 47, https://doi.org/10.1029/2019GL086045, 2020.

Brewer, P. J., Brown, R. J. C., Tarasova, O. A., Hall, B., Rhoderick, G. C., and Wielgosz, R. I.: SI traceability and scales for underpinning atmospheric monitoring of greenhouse gases, Metrologia, 55, S174–S181, https://doi.org/10.1088/1681-7575/aad830, 2018.

970   Brown, A. S., Milton, M. J. T., Brookes, C., Vargha, G. M., Downey, M. L., Uehara, S., Augusto, C. R., Fioravante, A. de L., Sobrinho, D. G., Dias, F., Woo, J. C., Kim, B. M., Kim, J. S., Mace, T., Fükö, J. T., Qiao, H., Guenther, F., Rhoderick, J., Gameson, L., Botha, A., Tshilongo, J., Ntsasa, N. G., Val'ková, M., Durisova, Z., Kustikov, Y., Konopelko, L., Fatina, O., and Wessel, R.: Final report on CCQM-K93: Preparative comparison of ethanol in nitrogen, Metrologia, 50, 08025–08025, https://doi.org/10.1088/0026-1394/50/1A/08025, 2013.

975   Collins, W. J., Derwent, R. G., Johnson, C. E., and Stevenson, D. S.: The oxidation of organic compounds in the troposphere and their global warming potentials, Clim Change, 52, 453–479, https://doi.org/10.1023/A:1014221225434, 2002.

Cooper, O. R., Parrish, D. D., Ziemke, J., Balashov, N. V., Cupeiro, M., Galbally, I. E., Gilge, S., Horowitz, L., Jensen, N. R., Lamarque, J. F., Naik, V., Oltmans, S. J., Schwab, J., Shindell, D. T., Thompson, A. M., Thouret, V., Wang, Y., and Zbinden, R. M.: Global distribution and trends of tropospheric ozone: An observation-based review,
980   https://doi.org/10.12952/journal.elementa.000029, 2014.

Van Dingenen, R., Dentener, F. J., Raes, F., Krol, M. C., Emberson, L., and Cofala, J.: The global impact of ozone on agricultural crop yields under current and future air quality legislation, Atmos Environ, 43, 604–618, https://doi.org/10.1016/j.atmosenv.2008.10.033, 2009.

Faiola, C. L., Erickson, M. H., Fricaud, V. L., Jobson, B. T., and Vanreken, T. M.: Quantification of biogenic volatile organic
985   compounds with a flame ionization detector using the effective carbon number concept, Atmos Meas Tech, 5, 1911–1923, https://doi.org/10.5194/amt-5-1911-2012, 2012.

Fischer, E. V., Jacob, D. J., Millet, D. B., Yantosca, R. M., and Mao, J.: The role of the ocean in the global atmospheric budget of acetone, Geophys Res Lett, 39, https://doi.org/10.1029/2011GL050086, 2012.

Fischer, E. V., Jacob, D. J., Yantosca, R. M., Sulprizio, M. P., Millet, D. B., Mao, J., Paulot, F., Singh, H. B., Roiger, A., Ries,
990   L., Talbot, R. W., Dzepina, K., and Pandey Deolal, S.: Atmospheric peroxyacetyl nitrate (PAN): A global budget and source attribution, Atmos Chem Phys, 14, 2679–2698, https://doi.org/10.5194/acp-14-2679-2014, 2014.

Galbally, I. E., Schultz, M. G., Buchmann, B., Gilge, S., Guenther, F., Koide, H., Oltmans, S., Patrick, L., Scheel, H.-E., Smit, H., Steinbacher, M., Steinbrecht, W., Tarasova, O., Viallon, J., Volz-Thomas, A., Weber, M., Wielgosz, R., and Zellweger, C.: Guidelines for Continuous Measurement of Ozone in the Troposphere, GAW Report No 209, Publication WMO-No. 1110, WMO, Geneva, 1–76 pp., 2013.

Goldstein, A. H. and Galbally, I. E.: Known and Unexplored Organic Constituents in the Earth's Atmosphere, Environ Sci Technol, 41, 1502–1800, https://doi.org/https://doi.org/10.1021/es072476p, 2007.

de Gouw, J. and Warneke, C.: Measurements of volatile organic compounds in the earth's atmosphere using proton-transfer-reaction mass spectrometry, Mass Spectrom Rev, 26, 223–257, https://doi.org/10.1002/mas.20119, 2007.

Grenfell, R. J. P., Milton, M. J. T., Harling, A. M., Vargha, G. M., Brookes, C., Quincey, P. G., and Woods, P. T.: Standard mixtures of ambient volatile organic compounds in synthetic and whole air with stable reference values, Journal of Geophysical Research Atmospheres, 115, D14302, https://doi.org/10.1029/2009JD012933, 2010.

Güttler, B. and Richter, W.: Traceability of chemical measurement results, Chimia (Aarau), 63, 619–623, https://doi.org/10.2533/chimia.2009.619, 2009.

Hoerger, C. C., Claude, A., Plass-Duelmer, C., Reimann, S., Eckart, E., Steinbrecher, R., Aalto, J., Arduini, J., Bonnaire, N., Cape, J. N., Colomb, A., Connolly, R., Diskova, J., Dumitrean, P., Ehlers, C., Gros, V., Hakola, H., Hill, M., Hopkins, J. R., Jäger, J., Junek, R., Kajos, M. K., Klemp, D., Leuchner, M., Lewis, A. C., Locoge, N., Maione, M., Martin, D., Michl, K., Nemitz, E., O'Doherty, S., Pérez Ballesta, P., Ruuskanen, T. M., Sauvage, S., Schmidbauer, N., Spain, T. G., Straube, E., Vana, M., Vollmer, M. K., Wegener, R., and Wenger, A.: ACTRIS non-methane hydrocarbon intercomparison experiment in Europe to support WMO GAW and EMEP observation networks, Atmos Meas Tech, 8, 2715–2736, https://doi.org/10.5194/amt-8-2715-2015, 2015.

Holzinger, R., Joe Acton, W. F., Bloss, W. W., Breitenlechner, M., Crilley, L. L., Dusanter, S., Gonin, M., Gros, V., Keutsch, F. F., Kiendler-Scharr, A., Kramer, L. L., Krechmer, J. J., Languille, B., Locoge, N., Lopez-Hilfiker, F., Materi, D., Moreno, S., Nemitz, E., Quéléver, L. L., Sarda Esteve, R., Sauvage, S., Schallhart, S., Sommariva, R., Tillmann, R., Wedel, S., Worton, D. D., Xu, K., and Zaytsev, A.: Validity and limitations of simple reaction kinetics to calculate concentrations of organic compounds from ion counts in PTR-MS, Atmos Meas Tech, 12, 6193–6208, https://doi.org/10.5194/amt-12-6193-2019, 2019.

Hu, L., Millet, D. B., Mohr, M. J., Wells, K. C., Griffis, T. J., and Helmig, D.: Sources and seasonality of atmospheric methanol based on tall tower measurements in the US Upper Midwest, Atmos Chem Phys, 11, 11145–11156, https://doi.org/10.5194/acp-11-11145-2011, 2011.

Iglesias-Suarez, F., Kinnison, D. E., Rap, A., Maycock, A. C., Wild, O., and Young, P. J.: Key drivers of ozone change and its radiative forcing over the 21st century, https://doi.org/10.5194/acp-18-6121-2018, 3 May 2018.

ISO 6145-10:2002 Gas analysis – Preparation of calibration gas mixtures using dynamic volumetric methods – Part 10: Permeation method, 1st edition, International Organization for Standardization (ISO), Geneva, Switzerland, 16 pp., 2002.
1025   https://iso.org/standard/25916.html, last access: 20 October 2023.

ISO 6145-4:2004 Gas analysis – Preparation of calibration gas mixtures using dynamic volumetric methods – Part 4: Continuous syringe injection method, 2nd edition, International Organization for Standardization (ISO), Geneva, Switzerland, 15 pp., 2004. https://iso.org/standard/36478.html, last access: 20 October 2023.

ISO 6145-8:2005 Gas analysis – Preparation of calibration gas mixtures using dynamic volumetric methods – Part 8: Diffusion
1030   method, 1st Edition, International Organization for Standardization (ISO), 19 pp., 2005. https://iso.org/standard/36480.html, last access: 20 October 2023.

ISO 6142-1:2015 Gas analysis – Preparation of calibration gas mixtures – Part 1: Gravimetric method for Class I mixtures, 1st edition, International Organization for Standardization (ISO), Geneva, Switzerland, 39 pp., 2015. https://iso.org/standard/59631.html, last access: 20 October 2023.

1035 ISO 6145-7:2018 Gas analysis – Preparation of calibration gas mixtures using dynamic methods – Part 7: Thermal mass-flow controllers, 3rd edition, International Organization for Standardization (ISO), 14 pp., 2018. https://iso.org/standard/73212.html, last access: 20 October 2023.

ISO 19229:2019: Gas analysis – Purity analysis and the treatment of purity data, 2nd Edition, International Organization for Standardization (ISO), Geneva, Switzerland, 18 pp., 2019. https://iso.org/standard/72010.html, last access: 20 October
1040   2023.

Jacob, D. J.: Heterogeneous chemistry and tropospheric ozone, Atmospheric Environment, 2131–2159 pp., https://doi.org/10.1016/S1352-2310(99)00462-8, 2000.

JCGM 100:2008 BIPM, IEC, IFCC, ILAC, ISO, IUPAC, IUPAP and OIML. Evaluation of measurement data – Guide to the expression of uncertainty in measurement (GUM). Joint Committee for Guides in Metrology (JCGM), 134 pp., 2008.
1045   https://www.bipm.org/documents/20126/2071204/JCGM_100_2008_E.pdf/cb0ef43f-baa5-11cf-3f85-4dcd86f77bd6, last access: 20 October 2023.

Khan, M. A. H., Cooke, M. C., Utembe, S. R., Archibald, A. T., Maxwell, P., Morris, W. C., Xiao, P., Derwent, R. G., Jenkin, M. E., Percival, C. J., Walsh, R. C., Young, T. D. S., Simmonds, P. G., Nickless, G., O'Doherty, S., and Shallcross, D. E.: A study of global atmospheric budget and distribution of acetone using global atmospheric model STOCHEM-CRI, Atmos
1050   Environ, 112, 269–277, https://doi.org/10.1016/j.atmosenv.2015.04.056, 2015.

Laj, P., Lund Myhre, C., Riffault, V., Amiridis, V., Fuchs, H., Eleftheriadis, K., Petäjä, T., Salameh, T., Kivekäs, N., Juurola, E., Saponaro, G., Philippin, S., Cornacchia, C., Alados Arboledas, L., Baars, H., Claude, A., De Mazière, M., Dils, B., Dufresne, M., Evangeliou, N., Favez, O., Fiebig, M., Haeffelin, M., Herrmann, H., Höhler, K., Illmann, N., Kreuter, A., Ludewig, E., Marinou, E., Möhler, O., Mona, L., Murberg, L.E., Nicolae, D., Novelli, A., O'Connor, E., Ohneiser, K., Petracca Altieri, R. M., Picquet-Varrault, B., van Pinxteren, D., Pospichal, B., Putaud, J. P., Reimann, S., Siomos, N., Stachlewska, I., Tillmann, R., Avoudouri, K.A., Wandinger, U., Wiedenshohler, A., Apituley, A., Comerón, A., Gysel-Beer, M., Mihalopoulos, N., Nikolova, N., Pietruczuk, A., Sauvage, S., Sciare, J., Skov, H., Svendby, T., Swietlicki, E., Tonev, D., Vaughan, G., Zdimal, V., Baltensperger, U., Doussin, J.-F., Kulmala, M., Pappalardo, G., Sorvari S. S., and Vana, M.: Aerosol, Clouds and Trace Gases Research Infrastructure – ACTRIS, the European research infrastructure supporting atmospheric science. Bull Am Meterol Soc., https://doi.org/10.1175/BAMS-D-23-0064.1, 2024.

Legreid, G., Lööv, J. B., Staehelin, J., Hueglin, C., Hill, M., Buchmann, B., Prevot, A. S. H., and Reimann, S.: Oxygenated volatile organic compounds (OVOCs) at an urban background site in Zürich (Europe): Seasonal variation and source allocation, Atmos Environ, 41, 8409–8423, https://doi.org/10.1016/j.atmosenv.2007.07.026, 2007.

Lelieveld, J. and Dentener, F. J.: What controls tropospheric ozone?, Journal of Geophysical Research Atmospheres, 105, 3531–3551, https://doi.org/10.1029/1999JD901011, 2000.

Leuenberger, M. C., Schibig, M. F., and Nyfeler, P.: Gas adsorption and desorption effects on cylinders and their importance for long-term gas records, Atmos Meas Tech, 8, 5289–5299, https://doi.org/10.5194/amt-8-5289-2015, 2015.

Matschat, R., Richter, S., Vogl, J., and Kipphardt, H.: On the way to SI traceable primary transfer standards for amount of substance measurements in inorganic chemical analysis, Anal Bioanal Chem, 415, 3057–3071, https://doi.org/10.1007/s00216-023-04660-4, 2023.

Miller, W. R., Rhoderick, G. C., and Guenther, F. R.: Investigating adsorption/desorption of carbon dioxide in aluminum compressed gas cylinders, Anal Chem, 87, 1957–1962, https://doi.org/10.1021/ac504351b, 2015.

Millet, D. B., Guenther, A., Siegel, D. A., Nelson, N. B., Singh, H. B., De Gouw, J. A., Warneke, C., Williams, J., Eerdekens, G., Sinha, V., Karl, T., Flocke, F., Apel, E., Riemer, D. D., Palmer, P. I., and Barkley, M.: Atmospheric Chemistry and Physics Global atmospheric budget of acetaldehyde: 3-D model analysis and constraints from in-situ and satellite observations, Atmos. Chem. Phys, 3405–3425 pp., https://doi.org/10.5194/acp-10-3405-2010, 2010.

Mills, G., Pleijel, H., Malley, C. S., Sinha, B., Cooper, O. R., Schultz, M. G., Neufeld, H. S., Simpson, D., Sharps, K., Feng, Z., Gerosa, G., Harmens, H., Kobayashi, K., Saxena, P., Paoletti, E., Sinha, V., and Xu, X.: Tropospheric ozone assessment report: Present-day tropospheric ozone distribution and trends relevant to vegetation, Elementa, 6, https://doi.org/10.1525/elementa.302, 2018.

Monks, P. S., Archibald, A. T., Colette, A., Cooper, O., Coyle, M., Derwent, R., Fowler, D., Granier, C., Law, K. S., Mills, G. E., Stevenson, D. S., Tarasova, O., Thouret, V., Von Schneidemesser, E., Sommariva, R., Wild, O., and Williams, M. L.: Tropospheric ozone and its precursors from the urban to the global scale from air quality to short-lived climate forcer, https://doi.org/10.5194/acp-15-8889-2015, 13 August 2015.

1085 Pascale, C., Guillevic, M., Ackermann, A., Leuenberger, D., and Niederhauser, B.: Two generators to produce SI-traceable reference gas mixtures for reactive compounds at atmospheric levels, Meas Sci Technol, 28, https://doi.org/10.1088/1361-6501/aa870c, 2017.

Persijn, S. T. and Baldan, A.: A new look at the sorption kinetics in reference gas standards, Meas Sci Technol, 34, https://doi.org/10.1088/1361-6501/ace9ee, 2023.

1090 Placet, M.: Emissions of ozone precursors from stationary sources: a critical review, Atmos Environ, 34, 2183–2204, https://doi.org/10.1016/S1352-2310(99)00464-1, 2000.

Pugliese, S. C., Murphy, J. G., Geddes, J. A., and Wang, J. M.: The impacts of precursor reduction and meteorology on ground-level ozone in the Greater Toronto Area, Atmos Chem Phys, 14, 8197–8207, https://doi.org/10.5194/acp-14-8197-2014, 2014.

1095 Rhoderick, G. C., Cecelski, C. E., Miller, W. R., Worton, D. R., Moreno, S., Brewer, P. J., Viallon, J., Idrees, F., Moussay, P., Kim, Y. D., Kim, D., Lee, S., Baldan, A., and Li, J.: Stability of gaseous volatile organic compounds contained in gas cylinders with different internal wall treatments, Elementa, 7, https://doi.org/10.1525/elementa.366, 2019.

Richter, W.: Recommendations on quantities, symbols and measurement units for publications in ACQUAL, Accreditation and Quality Assurance, 12, 497–498, https://doi.org/10.1007/s00769-007-0273-6, 2007.

1100 Seinfeld, J. H., Bretherton, C., Carslaw, K. S., Coe, H., DeMott, P. J., Dunlea, E.J., Feingold, G., Ghan, S., Guenther, A. B., Kahn, R., Kraucunas, I., Kreidenweis, S. M., Molina, M. J., Nenes, A., Penner, J.E., Prather, K. A., Ramanathan, V., Ramaswamy, V., Rasch, P. J., Ravishankara, A. R., Rosenfeld, D., Stephens, G., and Wood, R.: Improving our fundamental understanding of the role of aerosol-cloud interactions in the climate system. PNAS, 113, 5781–5790. https://doi.org/10.1073/pnas.1514043113, 2016.

1105 Schultz, M. G., Akimoto, H., Bottenheim, J., Buchmann, B., Galbally, I. E., Gilge, S., Helmig, D., Koide, H., Lewis, A. C., Novelli, P. C., Plass-Dölmer, C., Ryerson, T. B., Steinbacher, M., Steinbrecher, R., Tarasova, O., Tørseth, K., Thouret, V., and Zellweger, C.: The Global Atmosphere Watch reactive gases measurement network, Elementa, 3, 000067, 2015.

Schultz, M. G., Schröder, S., Lyapina, O., Cooper, O. R., Galbally, I., Petropavlovskikh, I., Von Schneidemesser, E., Tanimoto, H., Elshorbany, Y., Naja, M., Seguel, R. J., Dauert, U., Eckhardt, P., Feigenspan, S., Fiebig, M., Hjellbrekke, A. G., Hong, 1110 Y. D., Kjeld, P. C., Koide, H., Lear, G., Tarasick, D., Ueno, M., Wallasch, M., Baumgardner, D., Chuang, M. T., Gillett,

R., Lee, M., Molloy, S., Moolla, R., Wang, T., Sharps, K., Adame, J. A., Ancellet, G., Apadula, F., Artaxo, P., Barlasina, M. E., Bogucka, M., Bonasoni, P., Chang, L., Colomb, A., Cuevas-Agulló, E., Cupeiro, M., Degorska, A., Ding, A., Fröhlich, M., Frolova, M., Gadhavi, H., Gheusi, F., Gilge, S., Gonzalez, M. Y., Gros, V., Hamad, S. H., Helmig, D., Henriques, D., Hermansen, O., Holla, R., Hueber, J., Im, U., Jaffe, D. A., Komala, N., Kubistin, D., Lam, K. S., Laurila,

1115 T., Lee, H., Levy, I., Mazzoleni, C., Mazzoleni, L. R., McClure-Begley, A., Mohamad, M., Murovec, M., Navarro-Comas, M., Nicodim, F., Parrish, D., Read, K. A., Reid, N., Ries, L., Saxena, P., Schwab, J. J., Scorgie, Y., Senik, I., Simmonds, P., Sinha, V., Skorokhod, A. I., Spain, G., Spangl, W., Spoor, R., Springston, S. R., Steer, K., Steinbacher, M., Suharguniyawan, E., Torre, P., Trickl, T., Weili, L., Weller, R., Xiaobin, X., Xue, L., and Zhiqiang, M.: Tropospheric Ozone Assessment Report: Database and metrics data of global surface ozone observations, Elementa, 5,

1120 https://doi.org/10.1525/elementa.244, 2017.

Shao, M., Lu, S., Liu, Y., Xie, X., Chang, C., Huang, S., and Chen, Z.: Volatile organic compounds measured in summer in Beijing and their role in ground-level ozone formation, Journal of Geophysical Research Atmospheres, 114, https://doi.org/10.1029/2008JD010863, 2009.

Shrivastava, M., Cappa, C. D., Fan, J., Goldstein, A. H., Guenther, A. B., Jimenez, J. L, Kuang, C., Laskin, A., Martin, S. T.,

1125 Ng, N. L., Petaja, T., Pierce, J. R., Rasch, P. J., Roldin, P., Seinfeld, J. H., Shilling, J, Smith, J. N., Thornton, J. A., Volkamer, R., Wang, J., Worsnop, D. R., Zaveri, R. A., Zelenyuk, A., and Zhang, Q.: Recent advances in understanding secondary organic aerosol: Implications for global climate forcing, Rev Geophys, 55, 509–559, https://doi.org/10.1002/2016RG000540, 2017.

Simon, H., Reff, A., Wells, B., Xing, J., and Frank, N.: Ozone trends across the United States over a period of decreasing NOx

1130 and VOC emissions, Environ Sci Technol, 49, 186–195, https://doi.org/10.1021/es504514z, 2015.

Simon, L., Gros, V., Petit, J. E., Truong, F., Sarda-Estève, R., Kalalian, C., Baudic, A., Marchand, C., and Favez, O.: Two years of volatile organic compound online in situ measurements at the Site Instrumental de Recherche par Télédétection Atmosphérique (Paris region, France) using proton-transfer-reaction mass spectrometry, Earth Syst Sci Data, 15, 1947–1968, https://doi.org/10.5194/essd-15-1947-2023, 2023.

1135 Sternberg, J. C., Gallaway, W. S., and Jones, D. T. L.: The mechanism of response of flame ionization detectors, in: Gas Chromatography: Third International Symposium Held Under the Auspices of the Analysis Instrumentation Division of the Instrument Society of America, edited by: Brenner, N., Callen, J. E., and Weiss, M. D., Academic Press, New York and London, 231–267, 1962.

Stohl, A., Bonasoni, P., Cristofanelli, P., Collins, W., Feichter, J., Frank, A., Forster, C., Gerasopoulos, E., Gäggeler, H.,

1140 James, P., Kentarchos, T., Kromp-Kolb, H., Krüger, B., Land, C., Meloen, J., Papayannis, A., Priller, A., Seibert, P., Sprenger, M., Roelofs, G. J., Scheel, H. E., Schnabel, C., Siegmund, P., Tobler, L., Trickl, T., Wernli, H., Wirth, V., Zanis,

P., and Zerefos, C.: Stratosphere-troposphere exchange: A review, and what we have learned from STACCATO, Journal of Geophysical Research Atmospheres, 108, https://doi.org/10.1029/2002jd002490, 2003.

Tan, Z., Lu, K., Hofzumahaus, A., Fuchs, H., Bohn, B., Holland, F., Liu, Y., Rohrer, F., Shao, M., Sun, K., Wu, Y., Zeng, L.,
Zhang, Y., Zou, Q., Kiendler-Scharr, A., Wahner, A., and Zhang, Y.: Experimental budgets of OH, HO2, and RO2 radicals and implications for ozone formation in the Pearl River Delta in China 2014, Atmos Chem Phys, 19, 7129–7150, https://doi.org/10.5194/acp-19-7129-2019, 2019.

Tarasick, D., Galbally, I. E., Cooper, O. R., Schultz, M. G., Ancellet, G., Leblanc, T., Wallington, T. J., Ziemke, J., Liu, X.,
Steinbacher, M., Staehelin, J., Vigouroux, C., Hannigan, J. W., García, O., Foret, G., Zanis, P., Weatherhead, E.,
Petropavlovskikh, I., Worden, H., Osman, M., Liu, J., Chang, K. L., Gaudel, A., Lin, M., Granados-Muñoz, M., Thompson,
A. M., Oltmans, S. J., Cuesta, J., Dufour, G., Thouret, V., Hassler, B., Trickl, T., and Neu, J. L.: Tropospheric ozone assessment report: Tropospheric ozone from 1877 to 2016, observed levels, trends and uncertainties, https://doi.org/10.1525/elementa.376, 2019.

Volkamer, R., Sheehy, P., Molina, L. T., and Molina, M. J.: Oxidative capacity of the Mexico City atmosphere-Part 1: A
radical source perspective, Atmos Chem Phys, 10, 6969–6991, https://doi.org/10.5194/acp-10-6969-2010, 2010.

Wang, S., Hornbrook, R. S., Hills, A., Emmons, L. K., Tilmes, S., Lamarque, J. F., Jimenez, J. L., Campuzano-Jost, P., Nault,
B. A., Crounse, J. D., Wennberg, P. O., Kim, M., Allen, H., Ryerson, T. B., Thompson, C. R., Peischl, J., Moore, F., Nance,
D., Hall, B., Elkins, J., Tanner, D., Huey, L. G., Hall, S. R., Ullmann, K., Orlando, J. J., Tyndall, G. S., Flocke, F. M., Ray,
E., Hanisco, T. F., Wolfe, G. M., St. Clair, J., Commane, R., Daube, B., Barletta, B., Blake, D. R., Weinzierl, B., Dollner,
M., Conley, A., Vitt, F., Wofsy, S. C., Riemer, D. D., and Apel, E. C.: Atmospheric Acetaldehyde: Importance of Air-Sea Exchange and a Missing Source in the Remote Troposphere, Geophys Res Lett, 46, 5601–5613, https://doi.org/10.1029/2019GL082034, 2019.

Wild, O.: Atmospheric Chemistry and Physics Modelling the global tropospheric ozone budget: exploring the variability in current models, Atmos Chem Phys, https://doi.org/10.5194/acp-7-2643-2007, 2007.

WMO-BIPM: Metrology for Climate Action, Instruments and Observing Methods Report No. 142, Geneva, 88 pp., 2023.
https://library.wmo.int/idurl/4/66028, last access: 25 January 2024.

Worton, D. R., Moreno, S., Brewer, P. J., Li, J., Baldan, A., and van der Veen, A. M. H.: Bilateral comparison of primary reference materials (PRMs) containing methanol, ethanol and acetone in nitrogen, Accreditation and Quality Assurance, 27, 265–274, https://doi.org/10.1007/s00769-022-01513-y, 2022.

1170 Worton, D. R., Moreno, S., O'Daly, K., and Holzinger, R.: Development of an International System of Units (SI)-traceable transmission curve reference material to improve the quantitation and comparability of proton-transfer-reaction mass-spectrometry measurements, Atmos Meas Tech, 16, 1061–1072, https://doi.org/10.5194/amt-16-1061-2023, 2023.

Wu, C., Wang, C., Wang, S., Wang, W., Yuan, B., Qi, J., Wang, B., Wang, H., Wang, C., Song, W., Wang, X., Hu, W., Lou, S., Ye, C., Peng, Y., Wang, Z., Huangfu, Y., Xie, Y., Zhu, M., Zheng, J., Wang, X., Jiang, B., Zhang, Z., and Shao, M.:
1175 Measurement report: Important contributions of oxygenated compounds to emissions and chemistry of volatile organic compounds in urban air, Atmos Chem Phys, 20, 14769–14785, https://doi.org/10.5194/acp-20-14769-2020, 2020.

Xue, L. K., Wang, T., Gao, J., Ding, A. J., Zhou, X. H., Blake, D. R., Wang, X. F., Saunders, S. M., Fan, S. J., Zuo, H. C., Zhang, Q. Z., and Wang, W. X.: Ground-level ozone in four Chinese cities: Precursors, regional transport and heterogeneous processes, Atmos Chem Phys, 14, 13175–13188, https://doi.org/10.5194/acp-14-13175-2014, 2014.

1180 Yang, M., Nightingale, P.D., Beale, R., Liss, P.S., Blomquist, B., and Fairall, C.: Atmospheric deposition of methanol over the Atlantic Ocean, PNAS, 110, 20034-20039, https://doi.org/10.1073/pnas.1317840110.

Yang, Y., Shao, M., Wang, X., Nölscher, A. C., Kessel, S., Guenther, A., and Williams, J.: Towards a quantitative understanding of total OH reactivity: A review, Atmos Environ, 134, 147–161, https://doi.org/10.1016/j.atmosenv.2016.03.010, 2016.

1185 Young, P. J., Archibald, A. T., Bowman, K. W., Lamarque, J.-F., Naik, V., Stevenson, D. S., Tilmes, S., Voulgarakis, A., Wild, O., Bergmann, D., Cameron-Smith, P., Cionni, I., Collins, W. J., Dalsøren, S. B., Doherty, R. M., Eyring, V., Faluvegi, G., Horowitz, L. W., Josse, B., Lee, Y. H., MacKenzie, I. A., Nagashima, T., Plummer, D. A., Righi, M., Rumbold, S. T., Skeie, R. B., Shindell, D. T., Strode, S. A., Sudo, K., Szopa, S., and Zeng, G.: Pre-industrial to end 21st century projections of tropospheric ozone from the Atmospheric Chemistry and Climate Model Intercomparison Project
1190 (ACCMIP), Atmos Chem Phys, 13, 2063–2090, https://doi.org/10.5194/acp-13-2063-2013, 2013.

Young, P. J., Naik, V., Fiore, A. M., Gaudel, A., Guo, J., Lin, M. Y., Neu, J. L., Parrish, D. D., Rieder, H. E., Schnell, J. L., Tilmes, S., Wild, O., Zhang, L., Ziemke, J., Brandt, J., Delcloo, A., Doherty, R. M., Geels, C., Hegglin, M. I., Hu, L., Im, U., Kumar, R., Luhar, A., Murray, L., Plummer, D., Rodriguez, J., Saiz-Lopez, A., Schultz, M. G., Woodhouse, M. T., and Zeng, G.: Tropospheric Ozone Assessment Report: Assessment of global-scale model performance for global and regional
1195 ozone distributions, variability, and trends, Elem Sci Anth 6: 10, 49 pp, https://doi.org/10.1525/elementa.265, 2018.

Zborowska, A. G., MacInnis, C. Y., Ye, C. Z., and Osthoff, H. D.: On the photolysis branching ratio of methyl ethyl ketone, Atmos Environ, 254, 118383, https://doi.org/10.1016/j.atmosenv.2021.118383, 2021.

Zhang, H., Wu, S., Huang, Y., and Wang, Y.: Effects of stratospheric ozone recovery on photochemistry and ozone air quality in the troposphere, Atmos Chem Phys, 14, 4079–4086, https://doi.org/10.5194/acp-14-4079-2014, 2014.